LAPPEENRANTA UNIVERSITY OF TECHNOLOGY

LUT School of Energy Systems

LUT Mechanical Engineering

Yang Gao

RESEARCH ON PROPERTIES AND DESIGN METHODS OF CUSHION PACKAGING MATERIALS FOR CONSUMER ELECTRONICS

Examiners: Professor Kaj Backfolk

D.Sc. Katriina Mielonen

ABSTRACT

Lappeenranta University of Technology
LUT School of Energy Systems
LUT Mechanical Engineering

Yang Gao

Research on Properties and Design Methods of Cushion Packaging Materials for Consumer Electronics

Master's thesis

2018

126 pages, 81 figures, 14 table

Examiners: Professor Kaj Backfolk

Ph.D. Katriina Mielonen

Keywords: Packaging Material, Cushion Structure, Nonlinear, Simulation,

Transport package is very important in the logistic. The main tasks of transport package are to select proper cushioning material and obtaining reasonable structure.

For the consumer electronics packaging, EPS is the cushioning material used widely nowadays. But it cannot degrade and recycle, so lots of new cushioning materials appear. To use these new types of materials widely, it needs to do a lot of researches. This paper mainly discussed the property of the new cushioning materials and its design methods by simulation analysis and experimentation. Thus the cushion design methods of transport package are suggested.

The paper, firstly, studied the property of new cushioning materials through dynamic test, discussed the novel way to determine the cushioning curves. Then, the paper studied the dynamic response of the nonlinear materials to judge performance of nonlinear packaging and utilized the software of finite element analysis to simulate packaging drop response. Finally, the design methods of the cushion packaging are suggested.

ACKNOWLEDGEMENTS

This master thesis was carried out in Lappeenranta University of Technology, Finland. This work was lasting for long time due to my working reason, but finally I finished it.

Firstly, I want to express my highest respect to my supervisor, Professor Kaj Backfolk and Ph.D. Katriina Mielonen for giving me suggestions and encouragement to do my own research. They gave me valuable advice by rich experience. These suggestions opened my mind and helped me a lot.

I appreciate Professor Haiyan Song from Tianjin University of Science & Technology for providing the equipment for the dropping experiments and her assistants who help me to finish the experiments. I also appreciate the help from Professor Huapeng Wu, Dr. Xinxin Yu, Mr. Changyang Li, Mr. Xin Wang, Miss Xinwa Wang and Miss Dan Fu as well. They gave me strong power to face all the difficulties.

Fully love and many thanks to my parents and friends, without their supports, the thesis cannot be completed.

Yang Gao
Lappeenranta 22.05.2018

TABLE OF CONTENTS

LIST OF SYMBOLS AND ABBREVIATIONS

A	Force area [mm^2]
a_c	Maximum of acceleration before the product damage [m/s^2]
ba	The reloading curve
C	Buffer factor
C-σ_m	Cushioning coefficient - maximum stress curve
C-E	Cushioning coefficient - material specific energy curve
C-σ_m	Cushion coefficient maximum - stress curve
d	Backing limit deformation [mm]
d_b	The deformation limit of the material [mm]
F	Cushioning efficiency
F_0	Limit value of force F
f_n	Natural frequency
G_c	The product fragility [g]
G_m	Maximum acceleration
G_m - σ_{st}	The maximum acceleration - static stress curve
g	The acceleration of gravity [m/s^2]
k_0	The initial elastic coefficient
k	The elastic coefficient
oa	The initial loading curve
Pa	Calculated pressure unit [pa]
P_0	Ultimate pressure
R	The elastic coefficient increasing rate
W	The weight of impact [N]
(x)	Deformation quantity [mm]

ε	The total deformation [mm]
ε_e	Elastic deformation [mm]
ε_p	Plastic deformation [mm]

BKIN	Bilinear Kinematic Hardening Plasticity
DTM	Drop Test Module
FMI	Future Market Insight, consulting company
EPS	Expanded polystyrene
EPE	Expanded Polyethylene
EPU	Expanded Polyurethane
LCD	Liquid crystal display

1. INSTRUCTION

With rapid development of technology, consumer electronics market has dramatic increase. As an important link of whole value chain, the role of packages cannot be ignored. Under varieties of trends, there are higher materials and structures requirements for consumer electronics packaging. Packaging providers should help brand owners to build brand value and to gain more benefits with low cost. For this purpose, a complete design method for electronics products packaging is put forward.

1.1. Overview of consumer electronics

Electronic technology was emerging in the 19th century and has gotten rapid development in the 20th century with the progress of solid-state transistors and Large-Scale Integration With the continuous innovation of electronic technology, electronic products have achieved great development and been widely used. (Azzi 2012, Pp. 435-456.). Among various types of electronic products, consumer electronics account for major market share in this market, which also have the closest relations to people daily life.

According to a report carried out by FMI (Future Market Insight) which is a leading market intelligence and consulting company, the global consumer electronic market valued at 1,224.8 billion dollars in 2014 and is projected to reach 2,976.1 billion dollars by 2020, reflecting an annual growth rate at 15.4% during the forecast period. Increasing disposable income, expanding middle class population and all-pervasive internet penetration are prominent factors driving the growth of global consumer electronics market. (FMI 2015, Pp. 3-4.) In addition, strong government support in China has boosted the market growth. A t the first time, China surpassed the US and became the world's largest consumer electronics market in 2013 and will keep being this position in future as shown in Figure 1.

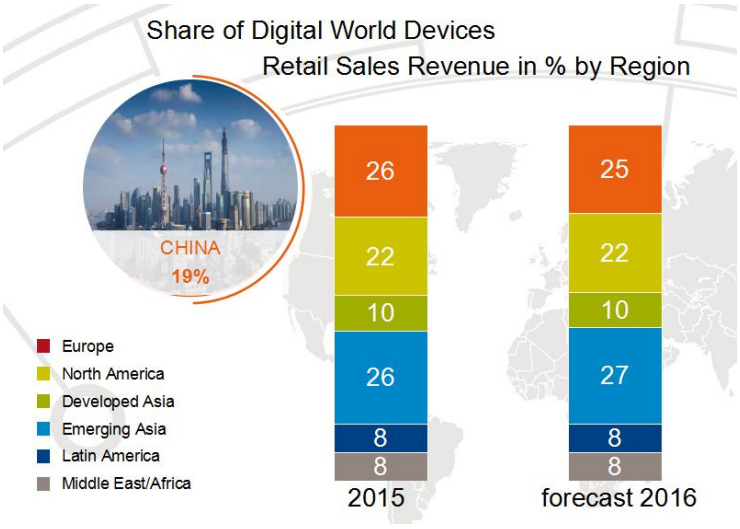

Figure 1. Share of Digital World Devices Retail Sales Revenue in % by Region (Smithers Pira 2015, p.148)

There are some well-known brands such as Apple, Samsung, Sony mainly located in a few countries like America, Japan and Korea, but the manufacturing and processing of these products are around the world. Major production bases are mainly located in east Asia, such as China and Singapore which can provide abundant low-cost labor. (Sodhi & Lee 2007, Pp.1430-1439.)

1.2. Overview of consumer electronics packaging

The market volume of consumer electronics is continually increasing, leading to a rapid development of its packaging. Packaging for consumer electronics is not only the indispensable last link for electronics industry, but also occupies an important position in the whole packaging industry. The packaging refers to various aspects such as materials, structures, decorations, transportation and so on.

For many brand owners, they usually outsource packaging design and manufacturing to professional packaging solution providers. Considering logistic cost, they prefer to choose adjacent packaging companies. There are many actors in the consumer electronics

packaging value chain in Figure 2, but packaging providers will play the most important role.

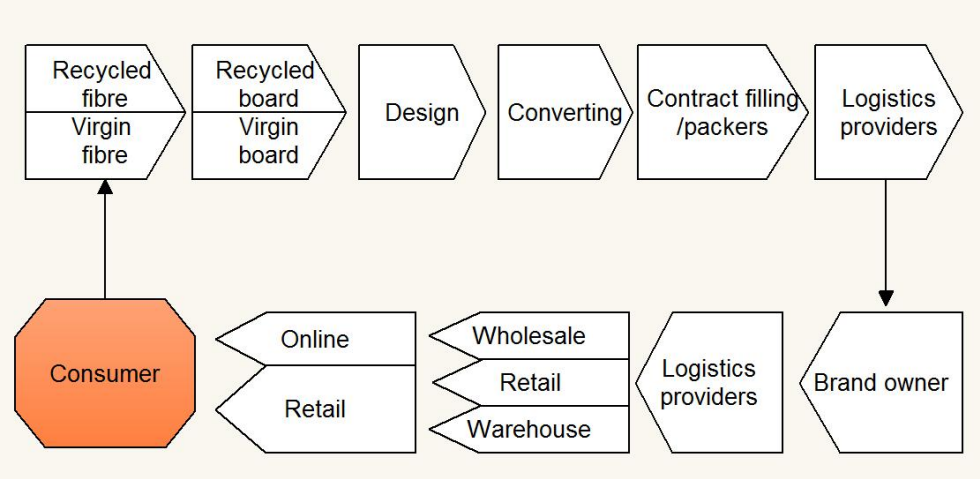

Figure 2. The consumer electronics packaging value chain (Olsson & Györei 2002, Pp.231-239)

Compared with other products, consumer electronics are more precise devices, thus they have higher requirements to avoid damage caused by possible vibrations or impacts from processes of handling, transportation and warehousing. So consumer electronics packaging should have high mechanical strength and good buffering performance to resist impacts or compression. Moreover, the convenience function and sales promotion function of packaging become more important, which put forward higher requirements for structure design, image, printing quality, packaging materials and processing adaptation. (Andrae & Andersen 2010, Pp. 827-836.)

As the packages for consumer electronics, there are some characteristics should be especially focused on. Firstly, most consumer electronics are highly integrated by large amounts of vulnerable electronic components which making very complex inner structures. External shocks and vibrations are easily to cause structure or function damage; thus they have high protective requirements. Secondly, consumer electronics generally cannot be long-term placed in humid environment, because moisture may enter inside of the product

and internal precise components will be affected by water resulting in short circuit or oxidation problems, so the packages should consider moisture-proof function. Similarly, these products cannot be exposed to dusty environment where tiny dust or oil particles can damage not only appearance of products but also their internal structures such as impeded current conduction in print circuit boards. (Zeng 2009, Pp.43-49). In addition, the static electricity is another important issue. It can breakdown internal precision parts and undermine working stability of electronic products. High static electricity will destroy whole product, causing very serious problem. Moreover, consumer electronics cannot withstand high temperature. Excessive temperature will reduce the lifetime of the products, or directly damage the circuit elements. When design packages for electronic products, all above points should be considered.

From structure perspective, the consumer electronics packaging can be generally divided into three defense lines: outer package, cushion package and inner package with dust-proof and anti-electrostatic plastic materials. Among these three lines, the most important one is the cushion package. For cushion package, foamed plastics are most common materials such as EPS (Expanded polystyrene), EPE (Expanded Polyethylene) and EPU (Expanded Polyurethane). The buffering principle of this kind of material is to use their deformations to absorb external shocks or vibrations. They generally have advantages of great cushion performance to effective protect inner products, low density to reduce transport cost, stable barrier properties to avoid moisture and good process ability to make complex shapes. Moreover, as mentioned above, dust and static electricity can cause serious damages to electronic components, thus using dust-proof and anti-electrostatic plastic as third defense is of great importance. Therefore, when design packages for consumer electronics, there is a need to overall consider on characteristics of products self, materials properties and cost, and structures rationality to achieve best protective effects. (Pecht 1991, Pp.128-132.)

1.3. Distribution environment

The distribution refers to whole processes of products from the manufacturers to consumers, a typical flow distribution as shown in Figure 3, consisting of the handling processes, transport process and warehousing process. Analyzing distribution environment is a part of the package design, its importance cannot be overrated but not be underestimated. Because if a package system wants to fulfill its protectiveness, it should have the ability to deal with complicated outside inputs from distribution environment and make these inputs keep in a safe level to avoid damage or failure.

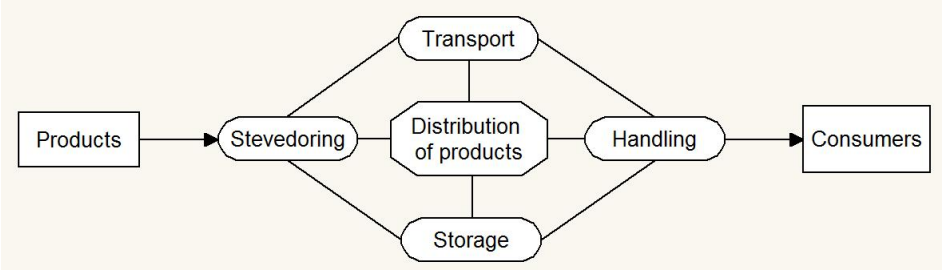

Figure 3. Typical distribution flow chart (Cai 2008, Pp. 22-25.)

Generally, there are two approaches for package designers to analyze distribution environment. One is using recorders to track the package and vehicle in transport to monitor what real issues happens to it. This method can gain plenty of valid data to describe distribution channel while its applicability is poor. Another one is collecting data from literature which can provide useful guidance and rules for package design, but this information is not often renewed or were made by experience. (Ok & Sasaki 2000, pp.45-53.)

The common external factors and reasons for damaged packages are shown in Table 1.

Table 1 External factors and reasons for damaged package (Peng 2006, Pp.137-145)

Factors	Specific form	Reasons for damaged packages
Mechanical factors	Shock	Falling, Tumbling, Jolting,Lateral impact, etc.
	Vibration	Vibrational excitation cause by Rough road, Rotor-engine/Rail joint/Sea wave
	Static pressure	Packaging strapping and tension forces when lifting, Stacking pressure
	Dynamic pressure	Resonance and collision between up and down goods due to carriers' vibration
Environmental factors	Temperature	Weakening of materials' buffering performance for thermal change
	Humidity	Materials' properties affected by Water-vapor diffusion
	Air pressure	High altitudes leading to temperature plummeting
	Light	Photo-degradation
	Water	Snow and Rain wet package, Splash in water transportation
	Salt fog	Salt particles' chemical corrosion
	Dust	Abrasion effects by sand particles
	Bio-tic factors	Micro-organism, Insect, Birds and Rats
	Radioactivity	Radioactive pollution
Human factors	Rough Handling	Workers' careless handling like throwing, improper operation of machines
	Steal	Forcible damage by prying and tamping

1.4. Cushioning materials for consumer electronics packaging

According to last section, cushioning materials is such the important parts that they need to be designed extremely carefully. Common cushion materials for consumer electronics include foam plastics, air cushions and paper-based materials. (Cai 2008, Pp.22-25.)

1.4.1. Common cushioning materials

Foam plastics

Foam plastics are widely used in buffering packaging design and among them, EPE, EPS and EPU, as shown in Figure 4,5,6 are most common selections for electronic products. The principle of foam plastics is to use their deformations to absorb external energy and to achieve the buffering effect. They generally have advantages of great buffering performance, low density and good workability. (Huang & Chen 2002, p.218)

There are some characteristics about them:

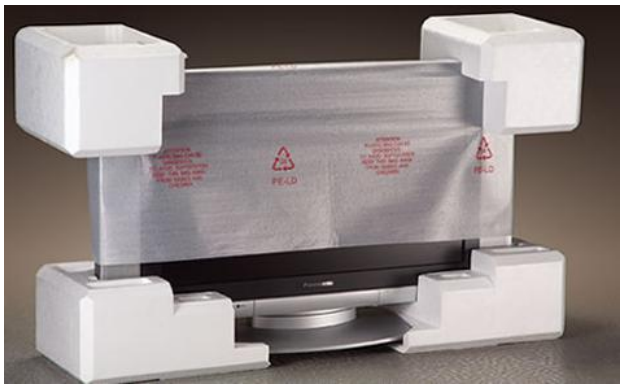

Figure 4. EPS cushion

- Good heat-durability; Closed-cell structure; Low water-absorbing quality; High mechanical strength; Low price.
- Liberate toxic gas when burning; weak recyclability.

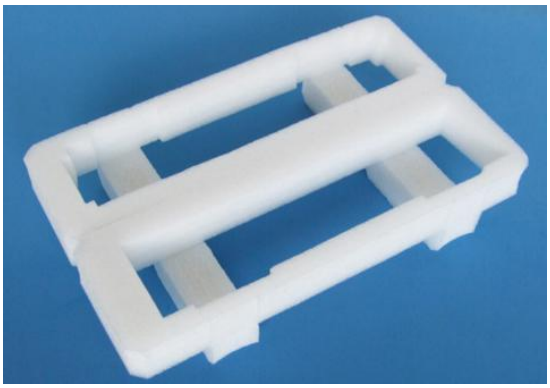

Figure 5. EPE cushion

- Good heat-durability; Chemical stability; good mechanical properties; Great flexibility and toughness; Easy to mold; Low price; Recyclable material.

Figure 6. EPU cushion

- Excellent flexibility, softness, elongation and compression strength; Good chemical stability and abrasion resistance
- High price

Air cushions

Air cushions, as shown in Figure 7 are made by special processes in which enclosing air between two layers of plastic films forms continuous bubbles whose shapes mainly include cylindrical type, semi-circular type and bell-shaped type. They have low density but excellent cushioning properties. Because a large amount of air is sealed, air cushions also have good flexibility and insulation. Besides, they do not absorb moisture and corrode inner products. But they are not suitable for heavy or load concentrated products with sharp objects, in case that bubbles are punctured and lose buffering function. (Liu & Song 2005, Pp.58-59.)

Figure 7. Air cushion

Corrugated board

Corrugated board is not only widely used for making boxes, but also a good choice for buffering materials as show in Figure 8. These successive thin U or V shape flutes between surface papers can absorb energy from external impacts and prolong products' duration time of withstanding shock pulse, providing good cushioning effects. With high mechanical strength and resilience, corrugated board can be easily to processed by die cutting or trimming into various cushions with different shapes and sizes. For different product kinds and shape characteristics, it should choose reasonable flute types and cushioning structures to optimal effects. Common structures include elastic type, folding type, elastic-folding type and corner type. Currently, more digital devices and small home appliances prefer using macro-corrugated board instead of form plastics to make cushions to enhance compressive strength and promote packaging grades. In short, it is a kind of recycled material that can meet buffering requirements with low cost. (Gao 2005, p. 68)

Figure 8. Corrugated board cushion

But not every aspect of corrugated board is perfect. It is not soft and easy to abrade the surface of the product with high appearance requirements. In addition, poor humidity resistance and weak overloaded resilience are shortcoming for corrugated board cushion. (Kirwan 2005, p.89).

Honeycomb board

Since honeycomb has good buffering performance, it can be used for cushion as corrugated cardboard, and honeycomb structure providing better flat crush resistance so that its cushioning properties is superior than corrugated board in several aspects. (Ma, Wang & Zou 2015, Pp.812-815.) According to different requirements of products, honeycomb cardboard can be made into corner pad, edge pad or surface pad as shown in Figure 9. For some special electronics, it can also be trimmed along with configurations of products by stamping, protecting and locating the devices properly. (Wang 2008, Pp.309-316.)

Figure 9. Honeycomb board cushion

In general, honeycomb board is more suitable for small and simple shape electronic products. Because disadvantages of this material are weak overloaded recovery ability and poor process ability due to its complex structures. Hence for large appliances, total production cost could be high, and some properties would not meet the requirements, such as poor humidity resistance.

Molded pulp

As a new branch of buffering packaging, molded pulp as shown in Figure 10 has a great development in recent years and widely application prospect due to a sharp rise of demand. It uses virgin or recycled pulp as base material, through unique technology and special additives to mold various geometrical shapes in preformed net molds which is based on figures of products. Because of kinds of structural units and their combinations, mold pulp has good cushion properties. Besides, lightweight, moisture-proof, anti-static, and fully recyclability makes it keep up with the trend of green packaging. (Eagleton, Marcondes 1994, Pp. 65-72.)

Figure 10. Molded pulp

Molded pulp can be used to fix product and its accessories and provide protection. But until now, common applications of it are limit to electronic products with low volume and weight such as smart phones, printers and set top boxes. For those heavy products with large size like washing machines, buffering effect is not very ideal.

1.4.2. Comparison of cushion materials in properties

This part lists common cushion materials and assesses their properties. According to buffering performance, grades from low to high are showed by 1-5 as shown in Table 2.

Table 2 Comparison of cushion materials in properties (Peng, 2006, p. 65)

Materials	EPS	EPE	EPU	Corrugated board	Honeycomb board	Molded pulp	Air cushion
Buffering Performance	3	4	5	2	1	1	5
Compressing stiffness	4	2	1	4	5	3	2
Volume	3	4	3	3	3	3	2
Tearing strength	2	3	3	2	1	2	3
Puncturing strength	2	3	3	2	1	2	3
Attrition for products	4	5	5	2	1	1	5
Size stability	3	4	4	2	2	2	1
Forming efficiency	5	3	4	3	1	5	4
Shape complexity	5	3	5	2	1	5	3
Appearance	3	4	5	2	1	2	4
Carbon emission	3	4	4	1	2	2	5
Recyclability	2	3	3	5	4	3	2
Disposal cost	2	2	2	5	4	4	2
Production cost	5	3	1	3	4	4	4
Material cost	5	3	1	4	5	5	4
Logistic cost	1	1	1	1	1	2	5

1.5. Valuable theory

There are some valuable theories can be used in this paper, they are fragility theory and damage boundary theory.

1.5.1. Fragility theory

During distribution process, breakages can cause value loss due to inadequate or improper packages. They have varieties of damaged forms, such as deformation of thin-wall shells,

rupture of fragile parts or failures of functions. So breakages can be regarded as circulation accidents, which are not only determined by inherent properties of the products (material, density, structure), but influenced by external distribution environment (handling, transport, storage). From packaging perspective, fragility as known as the degree of vulnerability, is used to describe strength when products undergo vibrations or shocks. The fragility reflects mechanical properties of the product and its ability to resist external impacts. When impact force which acts on the product exceeds the limit, structural damages or functional failures will happen. (Burgess 1988, Pp.5-10.)

Fragility is often represented by quantitative value, which is defined as the maximum acceleration that the product can bear before physical or functional damages occur. It is usually expressed by multiples of acceleration of gravity, shown as below equation (1):

$$G_c = \frac{a_c}{g} \tag{1}$$

where G_c is the product fragility, a_c represents maximum of acceleration before the product damage and g is the acceleration of gravity. It is worth to note that a_c is a constant determined by the product. The physical meaning of fragility is the capacity to withstand external shocks, the higher G_c value representing greater affordability for external force, vice versa. When the external impact acceleration reaches or exceeds its limit, breakage is inevitable. In order to guarantee safety, the product needs to be distributed under allowable fragility. A noteworthy thing is that in computer simulations, maximum acceleration during drop process is needed to more focused. (Burgess 1988, Pp.5-10.)

Fragility is not only an important indicator of product quality, but also a basic parameter for packaging cushion design. The fragility can be determined or estimated by the following four methods:

1) Trail method:

This method can use shock machine or drop tester, depending on the practical experimental conditions. As long as the test is carried out according to prescribed standards, the results basically correspond to the actual situations. Using experimental method to determine products fragility needs to destroy products, which is uneconomical for small batches or high value products. Besides, fragility for one product can be not always same in different directions, so different working conditions drop tests are needed to carry out separately. Considering these factors, the cost of this method is relatively high, thus it is applicable to low value products or mass-produced products. (Newton 1968, Pp.18-26.)

2) Analysis method:

This method is mainly used in the product development stage when experimentation cost is huge. A product is often made up of many components, and any damage of parts means failure of the entire product. Overall, some particularly vulnerable areas firstly appear in broken products, so the analysis method should analyze weaknesses of products, namely wearing parts, such as circuit boards or slender shaft. These vulnerable parts can be simplified as mechanical models like beams or plates, thus products fragility can be obtained by calculating the fragility of these mechanical models. (Newton 1968, Pp.18-26.)

3) Experiential method:

This method simplifies the package to a single-of-freedom linear system. When equivalent mass of package W and elastic coefficient k are known, natural frequency f_n can be determined. According to equation (2) below:

$$G_{\mathrm{m}} = \sqrt{\frac{2kH}{W}} = 2.837 f_n \bullet \sqrt{H} \tag{2}$$

Where drop height H and acceleration G_m have linear relationship, using H-G_m as coordinates, assigning different value to f_n.

$$f_n = \frac{1}{2\pi}\sqrt{\frac{k}{W}} \tag{3}$$

Taking advantage of this plot, allowable maximum acceleration (fragility) of products can be evaluated according to drop height of break accidents. While this theoretical fragility is estimated under condition with no damping and linear system, the results can be conservative. (Newton 1968, Pp.18-26.)

4) Analogy method

Many developed countries have made large amounts of experiments to get varieties of fragility for different products and listed certain reference standards. Table 3 is recommended fragility ranges from American military handbook MIL-HDBK-304. If there is no clear value for some products, it can be estimated by known products with similar structures.

Table 3. Fragility of Typical Products (Landrock 1995, Pp.215-216.)

Fragility (g)	**Products**
15-24	Missile Guidance System, Precision Aligned Test Equipment, Gyros, Inertial Guidance Platform
25-39	Mechanically Shock-Mounted Instruments, Digital Electronics Equipment, Altimeter, Airborne Radar Antenna
40-59	Aircraft Accessories, Most Solid-State Electronics Equipment, Computer Equipment
60-84	TV Receiver, Aircraft Accessories
85-110	Refrigerator, Appliance, Electra-Mechanical Equipment
110+	Machinery, Aircraft Structural Parts such as Landing Gear, Control Surface, Hydraulic Equipment

1.5.2. Damage boundary theory

Traditional fragility theory just uses critical acceleration of products to judge damage conditions. Except for magnitude of impact acceleration, the influence factors of damage

include the shape of shock pulse, duration time and velocity increment, which cannot be described only by acceleration, thus damage boundary theory has been proposed. This theory determines fragility from different perspective, and the damage boundary curve can be carried out through tests according to ASTM D3332. (Wang & Hu 1999, Pp.37-42.) The plot of results sets peaks accelerations as ordinate and increments of velocity as abscissa, and a curve divides coordinate plane into damaged area and undamaged area. Damage boundary curves of three typical pulses (Half-sine pulse, Final peak saw-tooth pulse and square wave pulse) are shown as Figure 11 (Wang 2001, Pp.149-157.). It can be see that square wave pulse is the most harmful shock type, thus tests commonly use this kind of pulse as shock source when distribution environment is unknown.

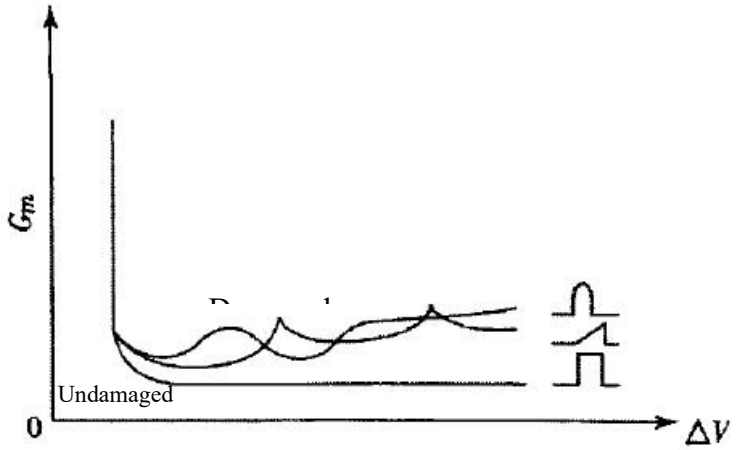

Figure 11. Damage boundary curve

From this plot, the external shock will cause damage when $G_m \geq G$ and $|\Delta V| \geq |\Delta V_C|$. While if the impact locates in undamaged area which is expressed as $G_m < G$ or $|\Delta V| < |\Delta V_C|$, the product will not be intact. Where G_m is maximum acceleration applied on the product, G is critical acceleration (fragility), ΔV is the velocity change and ΔV_c is critical velocity change.

1.6. Main work and research content

Based on the introduction of the cushioning packaging materials for consumer electronics and the analysis of theories and properties of the cushioning packaging, the theories of cushioning packaging and the design method will be researched in this paper. Through theoretical analysis modeling, numerical simulation, experimental analysis and other means to carry out comprehensive analysis and research, we strive to explore and establish a set of better cushioning package design system. The main contents of this paper are as follows:

The first chapter briefly discusses the important role of packaging for consumer electronics. According to listing requirements and distribution environments, it is pointed out that cushioning packaging is the most important parts for consumer electronics. Moreover, common cushioning materials and some valuable theories are listed. On this basis, the purpose of this paper, the means and methods of research and the problems to be solved are put forward.

The second chapter mainly studies the mechanical properties and buffer efficiency of the new environmental protection cushioning packaging materials. In the field of theoretical research, the transformation relationship between material buffer curves is deduced. Based on experimental verification, a novel method to determine the material's characteristic curve is established. This method can effectively reduce the test times of material buffering characteristics, save much resources, and provide foundation for improving of the material performance curve library in the current cushioning packaging design.

The third chapter is based on the stress-strain curve, the effect of the plasticity and viscosity of the material on the material buffering performance, a mechanical model of cushioning cushion is set up and the study of the impact response integral theory is carried out. The method to determine the acceleration time function of the response of the product

and the vulnerable parts under the nonlinear condition is given. The theoretical evaluation of the rationality of the selection of cushioning packaging materials is carried out by combining the theory of the shock brittle value and the breakage boundary curve of the cushioning package.

In the fourth chapter, the finite element theory and ANSYS/LS-DYNA software are used to simulate drop impact behavior of nonlinear transport packages. Through the test correction, a correct simulation model for the drop impact of the cushioning package is set up. This method can be used to evaluate the rationality of the design of the product cushioning transport package which is conducive to the rapid and accurate design of products and cushioning packaging. And it can provide a more suitable analysis method for the cushioning package design of complex conditions or valuable products.

The fifth chapter is verified by the method of experiment. First, the dynamic cushioning performance of the material is studied, and a set of buffer characteristic curves of the new environmental protection buffer material is drawn. Secondly, combined with the cushioning packaging structure of the specific product, we design the experimental scheme, then verified simulation’s correctness of the package through the package drop test, providing the basis for the revision of the numerical simulation model. Finally, the reliability and practicability of the finite element analysis are verified by comparing the drop test value of the package with the finite element simulation results.

In the sixth chapter, the application of nonlinear theoretical analysis and numerical simulation analysis of buffer packaging is discussed. The methods and steps of nonlinear theoretical analysis of cushioning packaging are illustrated by an example. The optimization process of the numerical simulation of the product cushioning packaging is proposed. Finally, the modern buffer packaging design system is summed up, and the traditional cushioning packaging design method is supplemented and perfected.

The seventh chapter summarizes the work and achievements of this article and puts forward the prospect of further research.

2. STUDY ON PROPERTIES OF CUSHIONING PACKAGING MATERIALS

2.1. Cushioning properties of materials

Mechanical shock and vibration phenomena can be seen throughout the circulation of transport packages. The purpose of using cushioning packaging material is to effectively absorb impact energy, and to control the impact acceleration that will be transferred to the built-in product in the range of product fragility, which is the first factor to be considered in choosing cushioning materials. However, it cannot be considered that the energy absorption will meet the requirements of cushioning. Different cushioning materials have different elastic properties, and their absorptive capacity to impact energy is also different. If the energy loss during the impact is not considered, and the mechanical energy of the maximum impact changes to the deformation energy of the cushioning material. Then the cushioning effect is better if the absorption energy is greater in the unit volume. (Miltz & Gruenbaum 1981, Pp.1010-1014.)

Suppose that the cushioning material is cubic and is subjected to an external force perpendicular to the area F, with an initial thickness of H, as shown in Figure 12. The deformation energy of the cushioning material under the action of force F is E:

$$E = \int_0^x F dx \tag{4}$$

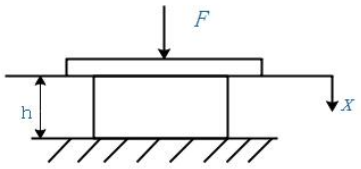

Figure 12. impact to the cushioning material

The absorbed energy per unit thickness of the cushioning material is $\frac{E}{h}$. (Guo & Zhang 2010, p.378)

The ratio of $\frac{E}{h}$ and F is defined as cushioning efficiency:

$$\eta = \frac{E/h}{F} = \frac{E}{Fh} \tag{5}$$

Cushioning efficiency is an important parameter to measure whether the cushioning package is reasonable or not. On the premise of protecting product requirements, the greater the cushioning efficiency, the more shock energy absorbed by the unit volume buffer material, the less the amount of cushioning material needed for the design.

Although the cushioning efficiency can reflect the cushioning properties of cushioning material but cannot be used directly in the design process. In practice, people usually use the reciprocal of buffer efficiency, which called the buffer factor, denoted as C.

$$C = \frac{1}{\eta} = \frac{Fh}{E} \tag{6}$$

2.2. Study on Cushioning Properties

The cushioning performance of materials is characterized by the cushioning characteristics of cushioning materials, which is an important basis for cushioning and anti-vibration packaging design. The common cushioning characteristic curves are as follows:

1. Cushioning coefficient - maximum stress curve (C- σ_m), cushioning factor - material specific energy curve(C-E) , these two curves can be obtained by static compression test.
2. The maximum acceleration - static stress curve (G_m - σ_{st}), the cushion coefficient maximum - stress curve(C- σ_m), these two curves can be obtained by dynamic compression test.

The above curves are drawn from the laboratory test results, and there is an internal relationship between them, so that they are collectively called material cushioning characteristics. The static compression test adopts the method of loading the material at low speed to obtain the compression force of the cushioning material and the deformation curve, which is a set of uniform compression process. However, in fact, as the material has viscous internal resistance, the greater the loading rate is, the greater the internal resistance of the material and the smaller the deformation of the material is. Therefore, the cushioning property of the material is related to the loading speed. The compression speed of dynamic compression test is usually tens of thousands of times of the static compression speed. The compression speed of dynamic compression test, which is a variable speed impact process, is usually tens of thousands of times of the static compression speed. In actual transportation, the product is often under dynamic loads, so that the dynamic compression test can better simulate the actual situation and reflect the cushioning characteristics of materials. (Guo & Zhang 2010, p.378)

The dynamic cushioning properties of the material are determined by dynamic compression tests. Dynamic compression test refers to the impact load of a cushioning material used in packaging to simulate the impact of the cushioning material when the package falls. The disadvantage of dynamic compression test is the large number of samples, long test time and high cost. To obtain a cushioning coefficient dynamic stress curve, more than 5 kinds of weight should be chosen, each quality should be less than 5 pieces and each sample should be impacted 5 times. The average value of the maximum acceleration of 4 times is taken as the maximum acceleration of the sample. The maximum acceleration of the 5 specimens is averaged as the maximum acceleration of the mass impact of the hammer (certain drop height and thickness sample). In other words, at least 25 specimens are used to shock 125 times, and these data are processed to obtain 5 discrete points, and then a dynamic stress curve of the cushion coefficient is fitted by the 5 discrete

points. But in order to test material properties better, dynamic compression test method should be adopted.

2.2.1. Testing principle of dynamic cushioning property of materials

In the cushioning material impact testing machine, using different weight of heavy hammer from a certain height along the guide column dropping impact sample, recording maximum impact acceleration, can obtain cushioning performance of buffer material through processing maximum acceleration data of multiple specimens. The impact process can be divided into three stages, as shown in Figure 13. (Sek, Minett, Rouillard & Bruscella 2000, Pp.249-255.)

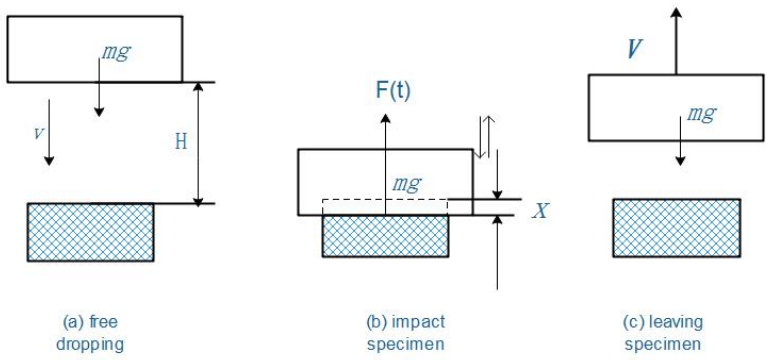

Figure 13. Packaging Drop Phase

The first stage is the free fall stage of the heavy hammer. At this stage, the heavy hammer is the free fall motion with the initial velocity being zero, and the acceleration is gravity acceleration g; The second stage is the sample stage of heavy hammer impact. This stage begins with the hammer impact sample until the hammer rises before leaving the sample. When the heavy hammer begins to contact the sample, the speed is $\sqrt{2gH}$. Then the velocity decreases gradually, and it moves upward until the specimen leaves the specimen when the velocity decreases to zero. At this stage, the weight has been touching the sample with the same displacement, velocity and acceleration as the sample; The third stage is the

stage of the heavy projectile from the sample. At this stage, the heavy hammer only affected by gravity leaves the specimen and the acceleration is gravity acceleration g.

The data acquisition system records changes in acceleration, taking the static stress $\sigma_{st} = \frac{W}{A}$ of buffer material as horizontal ordinate (W is the weight of impact table and weight, A is force area), and maximum impact acceleration G_m as ordinate, so curve of cushioning material can be obtained. Assumed that during the dynamic specimen process, the conservation of mechanical energy exists. When the cushioning material reaches the maximum strain, the gravitational potential energy of the heavy hammer at H height is equal to the deformation energy of the buffer material, that is

$$Ah\int_0^{\varepsilon_m} \sigma d\varepsilon = WH \tag{7}$$

Because

$$C = \frac{1}{\eta} = \frac{Fh}{E} = \frac{Fh}{\int_0^x Fdx} = \frac{Fh}{\int_0^{\varepsilon} A\sigma h d\varepsilon} \tag{8}$$

$$= \frac{Fh}{Ah\int_0^{\varepsilon} \sigma d\varepsilon} = \frac{A\sigma h}{Ah\int_0^{\varepsilon} \sigma d\varepsilon} = \frac{\sigma}{\int_0^{\varepsilon} \sigma d\varepsilon}$$

Under the impact of the heavy hammer, the maximum stress of the sample is

$$\sigma_m = \frac{G_m W}{A} \tag{9}$$

$$C = \frac{\frac{W}{A} G_m}{\frac{WH}{Ah}} = \frac{G_m h}{H} \tag{10}$$

In the equation (10), h is pad thickness.

$$\sigma_{st} = \frac{W}{A} \tag{11}$$

So

$$\sigma_m = \frac{G_m W}{A} = \sigma_{st} G_m \tag{12}$$

Put (11) into (9), so

$$\sigma_{st} = \frac{\sigma_m h}{CH} \tag{13}$$

Combine (13) and (11), one can obtain

$$\left.\begin{aligned} G_m &= \frac{CH}{h} \\ \sigma_{st} &= \frac{\sigma_m h}{CH} \end{aligned}\right\} \tag{14}$$

On the G_m - σ_{st} curve, H and h are constant. By using equation (10) and (12), each pair of coordinate values on the G_m - σ_{st} curve can be converted to the corresponding point in the C- σ_m coordinate graph, and the C- σ_m curve is obtained. (Yan & Xie 2010, Pp.27-31.)

2.2.2. Performance comparisons of common cushioning materials

This section mainly researches dynamic cushioning performance of single layer EPE with two different densities, and also make a comparison among some different common-used cushioning materials. According to characteristic curves, point out scope of applications of them.

Dynamic cushioning performance of single layer EPE material

According to the experimental data in table 9, the maximum acceleration-static stress curve of two density EPE gaskets can be plotted by using least square method of MATLAB, as shown in Figure 14. Figure 14 (A) and (B) are the maximum accelerations-static stress curve of the EPE220 gaskets at the drop height of 60era and 90era, respectively. Figure 14 (C) and (D) are the maximum accelerations-static stress curve of the EPE400 gaskets at the drop height of 60cm and 90era, respectively.

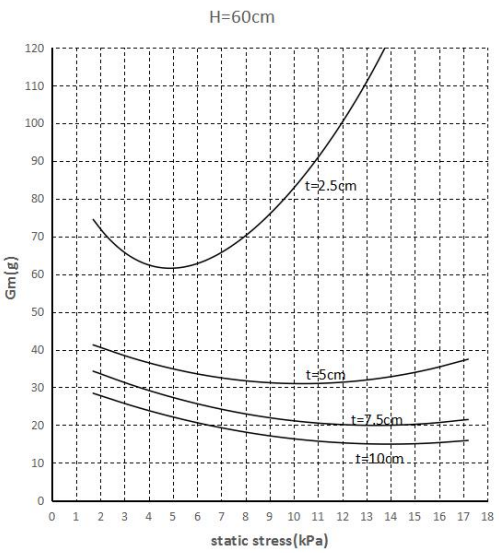

Figure 14. (A) $G_m - \sigma_{st}$ of EPE220 (H=60cm)

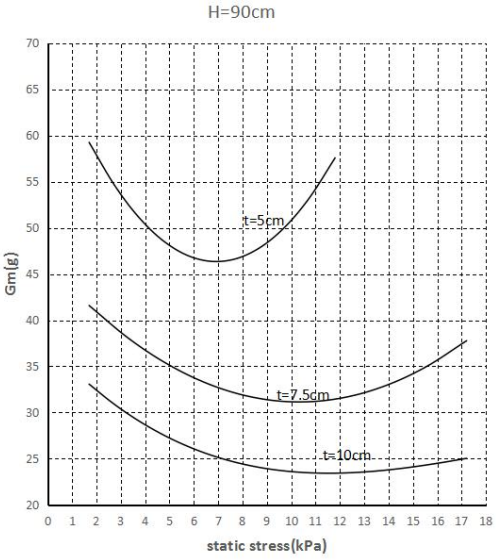

Figure 14. (B) $G_m - \sigma_{st}$ of EPE220 (H=60cm)

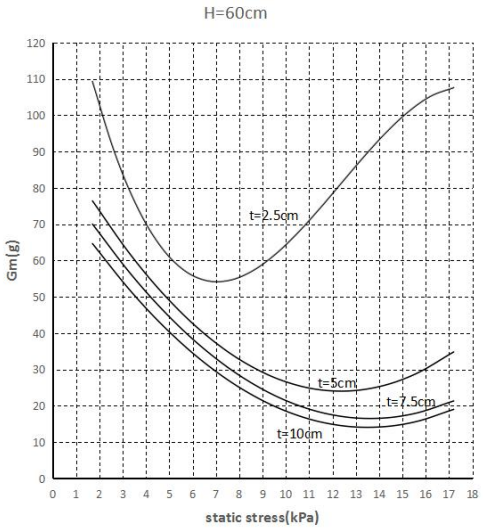

Figure 14. (C) $G_m - \sigma_{st}$ of EPE400 (H=60cm)

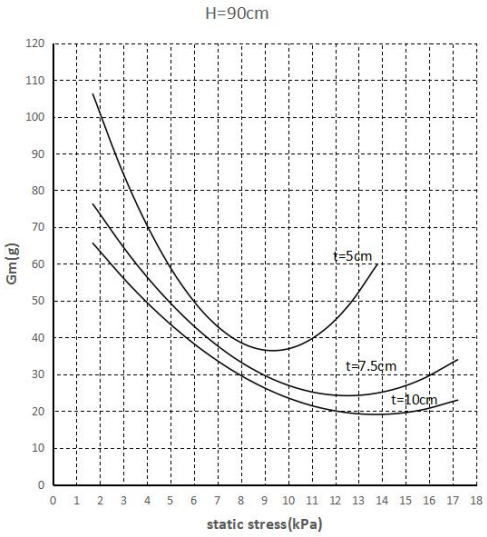

Figure14. (D) $G_m - \sigma_{st}$ of EPE400 (H=90cm)

As can be seen from Figure 14: the maximum acceleration-static stress curve of the EPE cushion is assumed to be in a concave valley shape and the opening is upward with only one extreme point. As for the liners of different thickness at the same maximum acceleration static stress curve under the drop height, with the increase of the gasket thickness, the minimum acceleration value decreased, the valley points right below the curve offset. Under the same impact, the greater the thickness of the liner, the greater the

absorption of energy, the better the buffer performance, so the smaller the acceleration produced by the impact. Moreover, the greater the thickness, the greater the static stress corresponding to the lowest point of the curve, and the greater the impact load can be under the same impact acceleration. As for maximum acceleration-static stress curve of foamed polyethylene gasket of the same thickness at different drop heights, with the drop height increasing, the minimum of the maximum acceleration has an upward trend, and the maximum acceleration of the gasket increases as the height of the drop increases in the same stress state.

Comparison of the performance of common cushioning packaging materials

To make an objective evaluation of the cushioning performance of environmental cushioning packaging materials, the dynamic characteristics of different type are comparatively studied. Taking the 2cm thickness of EPE220, AB-type and A-type corrugated board and honeycomb paperboard, dynamic compression test of materials is carried on with the dropping height of 40cm. The maximum acceleration-static stress curve of several materials is plotted as shown in Figure 15, according to the experimental data of Table 9 to Table 10-12.

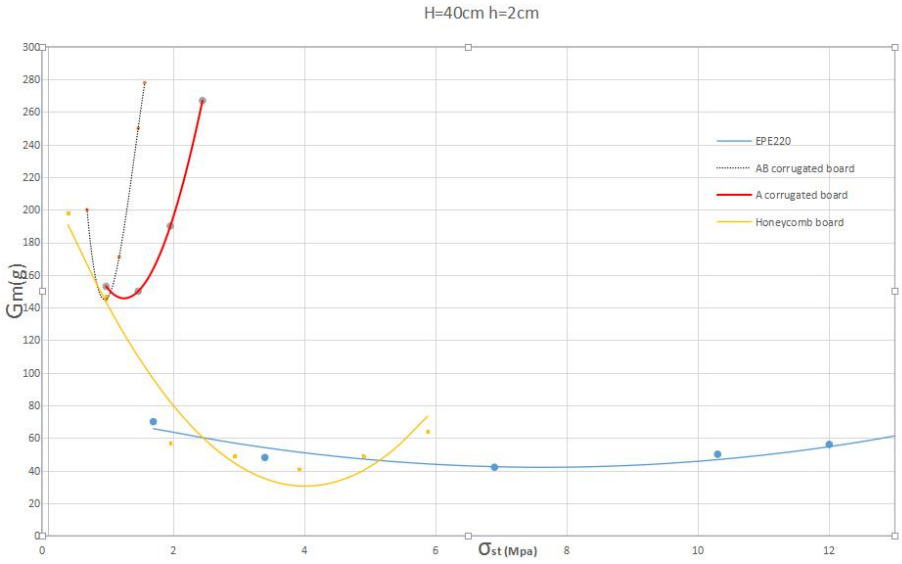

Figure 15. $G_m - \sigma_{st}$ of different materials (H=90cm, h=2cm)

It can be seen from Figures 15 and Table 10 to Table 12: Compared to other cushion pads, the minimum point of the $G_m - \sigma_{st}$ curve of the elastic corrugated paperboard is higher. That is, the minimum and maximum acceleration of the gasket is larger, and the static stress value of corrugated cardboard is smaller. As a result, the cushioning gasket of corrugated cardboard with smaller thicknesses are not suitable for products with less brittleness and greater weight. The maximum acceleration of honeycomb paperboard liner decreases significantly with the increase of static stress, and it can bear larger impact load. The $G_m - \sigma_{st}$ curve is on the left of EPE220 gasket, which shows that the impact load of honeycomb paperboard is smaller than that of EPE220 under the same impact acceleration. Under certain static stress range and same condition, the $G_m - \sigma_{st}$ curve of honeycomb paperboard is under the air cushion packing material and EPE220. For example, when the static stress is in the range of 2.2kPa to 5kPa,

At the same time stress, the same thickness, with a maximum acceleration drop height condition of honeycomb paperboard cushion than the values of EPE220 and air cushion packaging materials, good buffering performance. For example, when the static stress is in the range of 2.2kPa to 5kPa, the maximum acceleration value of honeycomb paperboard liner is smaller than that of EPE220, and the cushioning performance is better at the same time stress, the same thickness and the same height of fall conditions. The maximum acceleration of air cushion packing material decreases relatively with the increase of static stress. The minimum point of $G_m - \sigma_{st}$ curve of EPE cushion gasket is lower, the corresponding static stress value of the lowest point is larger, which can withstand relatively large impact load, and has good buffering performance and wide application range.

2.3. Research on determination method of cushion characteristic curve

Cushion characteristic curves are important properties for packaging materials. According to research their relationships and determination methods of these characteristic curves, it can gain the performance of the packaging materials.

2.3.1. Relationship between material cushioning characteristic curve

When we design cushion packing, we can use either the maximum acceleration-static stress curve to design, or we can design the maximum stress curve with the cushion coefficient. From equation (15), we can see that if σ_m is known, C can be obtained on the $C-\sigma_m$ curve of the material. Therefore, both G_m and σ_{st} are just functions of σ_m after both H and H are fixed. It can be seen that the equation(15) is a parameter equation when taking σ_m as the parameter which determines the functional relationship between G_m and σ_{st} . When the $G_m-\sigma_{st}$ curve is drawn, the height of the drop is first fixed, the thickness of the liner is varied, and the parameter equation is established. Each of the pads has a equation and a corresponding curve. When drawing the $G_m-\sigma_{st}$ curve, fix the drop height first, adopt different liner thickness to establish parameter equation. For each pad thickness, there is an equation and a corresponding curve. At the same drop height, the $G_m-\sigma_{st}$ curve is a curve cluster and the amount of pad thicknesses are taken, the amount of curve are there on this curve cluster. The $G_m-\sigma_{st}$ curves are different from different drop heights. After the H is fixed, the greater the H value, the smaller the G_m minimum, and the greater the σ_{st} value corresponding to this minimum. Equation (14) shows that the $C-\sigma_m$ curve of the material can be plotted by the $G_m-\sigma_{st}$ curve. Thus, the $C-\sigma_m$ curve and the $G_m-\sigma_{st}$ curve can be transformed each other, and the $G_m-\sigma_{st}$ curve is not another independent curve of the material buffering characteristics. In the

dynamic experiments, as long as the thickness of the sample is greater than 2.5cm, a material has only one $C-\sigma_m$ curve corresponding to it, while the $G_m-\sigma_{st}$ curve is not the same. There is one drop height in a graph and one thickness of a curve in a graph. Strictly speaking, it is necessary to use numerous $G_m-\sigma_{st}$ curves to describe the buffering characteristics of materials completely, that is to say, a $C-\sigma_m$ curve of cushion materials can be obtained with numerous $G_m-\sigma_{st}$ curves.

2.3.2. Determination method of material cushioning characteristic curve

According to equation (14), it can be deduced:

$$C = G_m \frac{h}{H} \tag{15}$$

$$\sigma_m = \frac{\sigma_{st} CH}{h} \tag{16}$$

From the above analysis, we can see that there is only one $C-\sigma_m$ curve for a material, and there are numerous $G_m-\sigma_{st}$ curves corresponding to it. Therefore, take a spot (C, σ_m) at the $C-\sigma_m$ curve, the spot of (G_{m1}, σ_{st1}) must be existed at the $G_m-\sigma_{st}$ curve, which satisfies:

$$C = G_{m1} \frac{h_1}{H_1} \tag{17}$$

$$\sigma_m = \frac{\sigma_{st1} CH_1}{h_1} \tag{18}$$

The spot (G_{m2}, σ_{st2}) can be existed at the $G_m-\sigma_{st}$ curve, which satisfies:

$$C = G_{m2} \frac{h_2}{H_2} \tag{19}$$

$$\sigma_m = \frac{\sigma_{st2} CH_2}{h_2} \tag{20}$$

Combine the equation (17), (19) and (18), (20), it can be deduced:

$$G_{m1}\frac{h_1}{H_1}=G_{m2}\frac{h_2}{H_2}\quad,\quad\frac{\sigma_{st1}CH_1}{h_1}=\frac{\sigma_{st2}CH_2}{h_2} \tag{21}$$

So

$$G_{m2}=\frac{H_2h_1}{H_1h_2}G_{m1} \tag{22}$$

$$\sigma_{st2}=\frac{H_2h_1}{H_1h_2}\sigma_{st1} \tag{23}$$

Therefore, when the drop heights are same, the $G_m-\sigma_{st}$ curve of different thickness of the gaskets satisfy:

$$\left.\begin{aligned}G_{m2}&=\frac{h_2}{H_1}G_{m1}\\ \sigma_{st2}&=\frac{h_2}{H_1}\sigma_{st1}\end{aligned}\right\} \tag{24}$$

When the thickness of the gaskets is same, the $G_m-\sigma_{st}$ curve of different drop height satisfy:

$$\left.\begin{aligned}G_{m2}&=\frac{H_2}{H_1}G_{m1}\\ \sigma_{st2}&=\frac{H_2}{H_1}\sigma_{st1}\end{aligned}\right\} \tag{25}$$

According to the above theoretical deduction, as long as we know any $G_m-\sigma_{st}$ curve from gasket $G_m-\sigma_{st}$ curve cluster, we can draw other $G_m-\sigma_{st}$ curves with different thicknesses and different drop heights. This can greatly reduce the number of tests, manpower and financial costs, and facilitate the application of $G_m-\sigma_{st}$ St curves.

There are some the dynamic compression test values of EPE and EPS foam gaskets are illustrated below.

According to the test data of test number EPE22060 in Table 9, the $G_m - \sigma_{st}$ curve can be drawn at a drop height of 60cm and a thickness of 2.5cm. According to equation (24), when fix gasket drop height and change pad thickness only, the $G_m - \sigma_{st}$ curve of the thickness of 5cm, 7.5cm and 10 cm can be obtained by computer, as shown in Figure 15. The "orange dot" in the figure is test point of maximum acceleration and static stress of cushion under corresponding thickness.

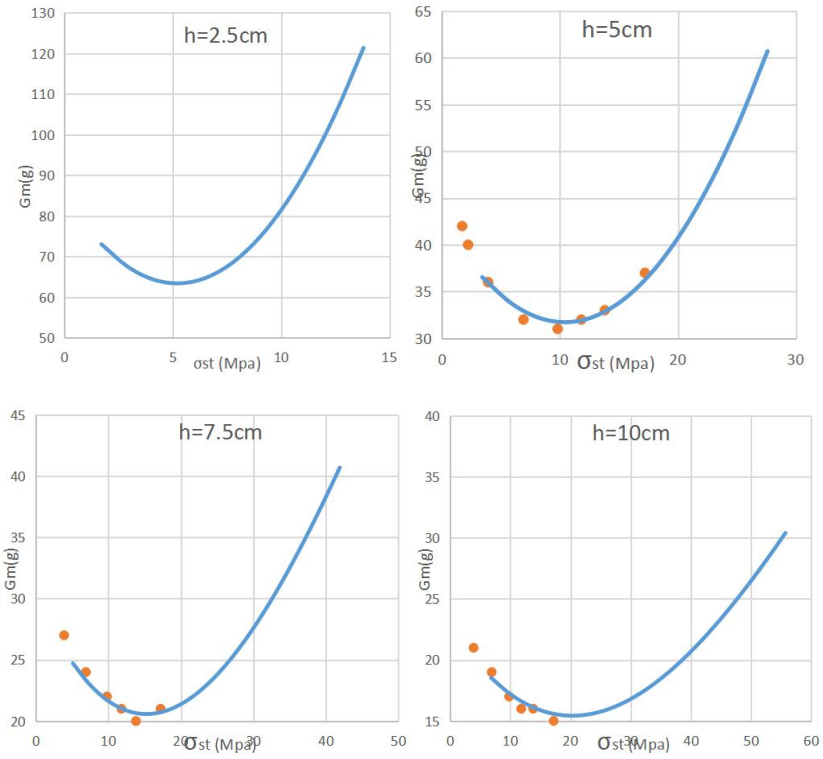

Figure 15. $G_m - \sigma_{st}$ curves of EPE220

Similarly, according to the test data of test number EPE22060 in Table 9, the $G_m - \sigma_{st}$ curve can be drawn at a drop height of 60cm and a thickness of 5cm. According to equation (25), when fix pad thickness and change gasket drop height only, the $G_m - \sigma_{st}$ curve of the drop height of 90 cm can be obtained by computer, as shown in

Figure 16. The “black dot” in the figure is test point of maximum acceleration and static stress of cushion under drop height of 90cm.

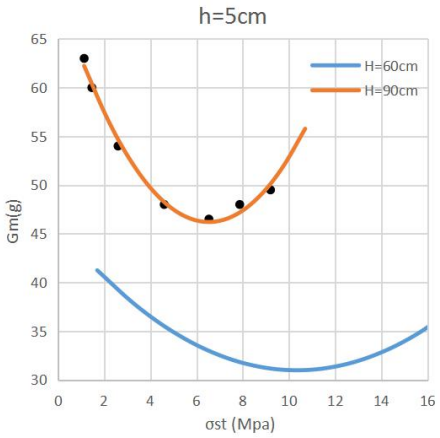

Figure 16. $G_m - \sigma_{st}$ curves of EPE220 (h=5cm)

As can be seen from Figure 15 and 16, considering the error of the test itself, the error between the $G_m - \sigma_{st}$ curve of the material obtained by the method mentioned above and the actual test value is within the acceptable range. The method can meet the requirement of engineering design precision under the condition of reducing the number of tests. If the original test curve is connected by more test points, then the calculated buffer curve is more accurate, which is more consistent with the actual curve.

If the method of dynamic compression test is adopted, a cushion material needs to be tested with 25 specimens at least 125 times, and 5 discrete points are obtained, and then a $G_m - \sigma_{st}$ curve can be fitted by the 5 discrete points. Moreover, it is necessary to use numerous $G_m - \sigma_{st}$ curves to describe fully the cushioning properties of materials. Thus, it is an extremely complicated job to determine the cushioning property curve test of cushion materials. In addition, the cushioning characteristic curve must be redetermined every time the thickness of the cushion material is changed or the drop height in the circulation environment is changed. Because the curve is necessary for cushioning

packaging design and selecting cushioning packaging materials, the new method can be used to obtain the $G_m - \sigma_{st}$ curve of the expected thickness of the liner or the height of the drop, when the actual human, financial, material resources cannot meet the requirements.

2.4. Conclusion

This chapter discussed properties of new environmental cushioning materials, and the cushioning characteristics of the materials are obtained. Under the same conditions, the cushioning properties of several commonly used environmental cushioning packaging materials are compared and analyzed; the relation between material cushioning characteristic curve is deduced, and a new method to determine cushioning curve of packing cushion material is established. Finally, the correctness of the experiment is verified. This method can greatly reduce the manpower and material resources needed to draw the material cushioning characteristic curve and set a solid designed basis of cushioning material and the improvement of the material performance curve library.

3. STUDY ON IMPACT THEORY OF NONLINEAR CUSHIONING PACKAGING

3.1. Basic mechanical properties of cushion materials

The mechanical property of cushion material refers to the force and deformation, which are mainly studied according to the stress-strain curve of materials. According to rheology, cushioning material belongs to visco-elastic material, which is a substance that is assumed to consist of three elements of elasticity, viscosity, and plasticity.

3.1.1. Elasticity

The material will deform under the action of external force, and the original state of the material can be recovered after removing the external force, which is called elasticity. Deformation of an object is prevented by an external force, which seeks to restore the original state. When the external force is removed, the internal stress which is elasticity (restoring) force disappears with the restoration of the state. When the external force increases, the elastic limit, that is, when the external force is removed, the material can completely recover the strain limit of its original state. (Muskhelishvil 2013, Pp.161-165.)

The actual elasticity of the cushion material, which the stress and the stress strain relationship, is quite complex and depends not only on the material, but also on the specific structure, loading mode, temperature, and so on. To facilitate the study, the stress-strain curves of simple compression under standard temperature are simplified, which are classified two types, linear and non-linear.

(1) Linear elastic materials.

These materials comply with Hooke's law in use, i.e., their range of use does not exceed their elastic boundaries, i.e., materials with a wide elastic limit. The force and deformation curves of this kind of material are linear, as shown in Figure 17, and the relation between force (F) and deformation (x) can be expressed as: $F = kx$

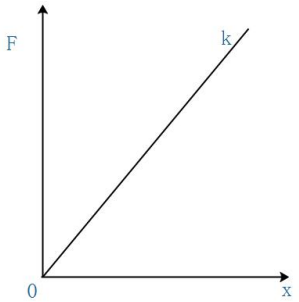

Figure 17. Linear Elastomer Material

For a linear elastic material, its load and deformation curve are straight. However, most of the cushioning packaging materials used in practical engineering belong to nonlinear elastic bodies. Only the cushioning material deforms very little, or require the calculation accuracy is not high, it is possible to approximate all cushion materials as linear elastic bodies. A typical linear elastic material is a metallic spring. (Muskhelishvil 2013, Pp.161-165.)

(2) Nonlinear elastic materials.

Nonlinear elasticity has three forms of equation, tangent, hyperbolic and irregular (i.e., the front section is hyperbolic tangent, and the latter is like the combined form of tangent shape) and so on.

A. Cubic equation elastomer material.

The force and deformation curve of this kind of material is cubic equation, as shown in Figure 18. The relation between force (F) and deformation quantity (x) can be expressed as:

$$F = k_0 + rx^3 \tag{26}$$

In the equation, k_0 is the initial elastic coefficient, and r is the elastic coefficient increase rate. The cubic equation type is very close to linear in small deformation. Unlike linear elastic materials, when the deformation goes up, with rise of absolute value of elastic coefficient, the speed at which an elastic line deviates from a line is bigger, the corresponding material will become softer or harder. The cubic equation elastomer material is the main representative of the suspension package of composite springs, in addition, wood chips, acetate fibers, silk, coating fiber, plastic silk and other materials are also three times the nature of functional type.

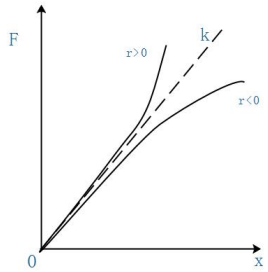

Figure 18. Cubic Equation Elastomer Material

B. Tangent elastomer material

The force - deformation curves of these materials are tangent equations, as shown in Figure 19. The relation between force (F) and deformation quantity (x) can be expressed as:

$$F = \frac{2k_0 d_b}{\pi} tg \frac{\pi x}{2d_b} \tag{27}$$

In the equation, k_0 is the initial elastic coefficient and d_b is the deformation limit of the material. Plastic, sponge rubber, latex, sponge, shredded paper, cotton and other materials all have the property of tangent equation. (Muskhelishvil 2013, Pp.161-165.)

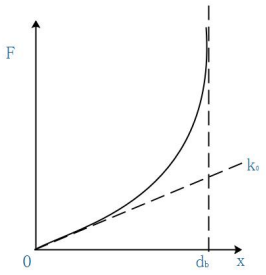

Figure 19. Tangent Elastomer Material

C. Hyperbolic tangent elastomer material

The force - deformation curves of these materials are double tangent, which is the elastic limit of smaller materials in a wide range of typical performance. As shown in Figure 20, the relation between force (F) and deformation quantity (x) can be expressed as:

$$F = F_0 th \frac{k_0 x}{F_0} \tag{28}$$

In the equation, k_0 is the initial elastic coefficient, F_0 is the limit value of force F, when $x \to \infty$ and $F \to F_0$. In the range allowed by deformation, no matter how deformation increases, the force F is limited to the F_0 range. Such materials are used as cushioning packaging materials, the delivery to the internal product of the force can be limited to less than the product itself to withstand the ability to protect the product in the impact process. Materials of this nature include corrugated cardboard, honeycomb paperboard, foam plastics, etc.

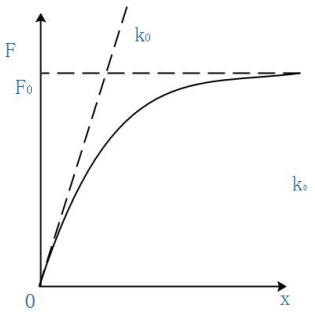

Figure 20. Hyperbolic Tangent Elastomer Material

D. Abnormity elastomer material

This kind of material is obviously different from the above four materials, and the relation between force and deformation can be shown in Figure 21. With one or more mathematical expressions, it is difficult to express the relationship between force and deformation, and polymeric foams belong to this kind of material.

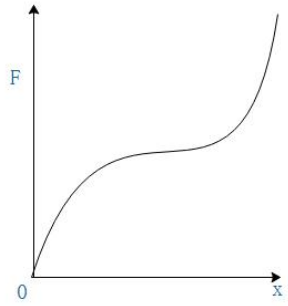

Figure 21. Abnormity Elastomer Material

For nonlinear elastic materials, the slopes of the points on the deformation curve are different, so the elastic module E and k of each point are different. If the elastic modulus of the material increases with the increase of the deformation, the gasket becomes more and more rigid with the increase of deformation, such material is called hard elastic material. Or if the elastic modulus of the material decreases with the increase of the deformation, the gasket becomes more and more soft with the increase of deformation, such material is called soft elastic material. The stress-strain curves of some materials are front soft back hard, such materials are called soft and hard composite elastic materials, as shown in Figure22. (Hill 1998, Pp.68-72.)

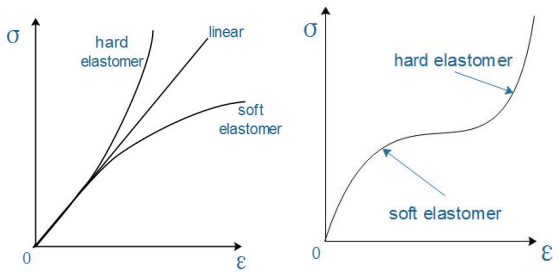

Figure 22. Nonlinear elastomer materials

3.1.2. Plasticity

A solid can behave elastically in external forces within its elastic limit, but as soon as it exceeds the limit, it will flow and cause permanent deformation or destruction, which is called plasticity. On the stress-strain curve, when the load is below the elastic limit and the line is unloaded, the original point can be returned along the original path without residual deformation. However, when the load exceeds the elastic limit into the curve and unloading does not return along the original route, residual deformation remains after all the load is removed. Although this deformation has been removed a little over time, most of the deformation will never recover, which is called permanent deformation. (Hill 1998, Pp.68-72.)

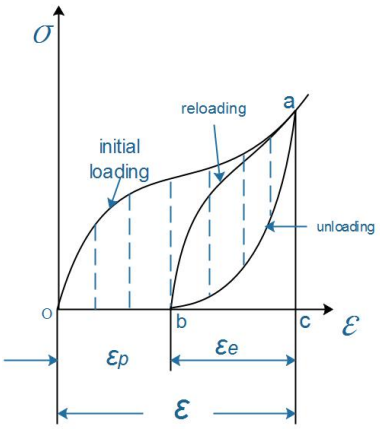

Figure 23. Elastic and Plastic Distortion of Material

Since the material is plastic, the total deformation ε of the material under arbitrary force includes elastic deformation ε_e and plastic deformation ε_p. When removing the load material residual deformation, stress and strain cannot be returned to the origin, if loading, the loading curve is no longer at the beginning of the loading curve. As shown in Figure 23, oa is the initial loading curve, and ba is the reloading curve. When the loading is also loaded to the a point a, the corresponding deformation at the initial load is ε, and then the corresponding deformation is ε_e, which is $\varepsilon_e < \varepsilon$. So, the material hardens when it is loaded again.

3.1.3. Viscosity

Cushioning materials, especially foam plastics, produce resistance when subjected to vibration and shock. This resistance is called internal resistance of materials. It is a resistance to the deformation of the material itself, caused by internal friction and the shape of the internal structure. Internal resistance and the speed of loading are inseparable, the greater the loading speed is, the greater the internal resistance is. If the load speed is zero, the internal resistance will disappear. This property of material is called viscosity, and its internal resistance is called viscous internal resistance. The effect of viscous internal resistance is like damper, so the damper is used as the mechanical model of material viscosity. As shown in Figure 24, it is generally shown that the resistance is proportional to the speed of motion, that is, linear damping. (Chapman & Cowling 1970, Pp.125-128.)

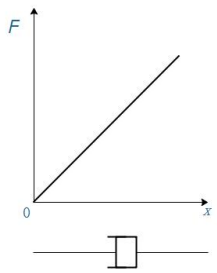

Figure 24. Viscosity

To highlight influence of viscosity on the mechanical properties of materials and neglect the plasticity, the foam plastics are usually abstracted into ideal visco-elastic material in Figure 25(a). The loading rate is only 10-15mm/min, so the compression test is called static loading test. As the loading speed is too small, the viscosity of the material is not obvious, and the stress-strain curve obtained is close to the ideal elastic material, such as ob in Figure 25(c). Its characteristic is that the loading and unloading curves coincide, the loading curve starts from the origin, and the unloading curve goes back to the origin. When the package is subjected to vibration shock, the product acts on the cushioning material approximately to the compression test, but its loading speed in Figure 25(b) is much larger than that of the static load test, and the stress-strain curve is also different from the static

load curve. In this case, the viscosity of the material is particularly prominent. When loading, the internal force of the material is the sum of the elastic force and the viscous resistance, so the loading curve oab is above the static load curve ob, as shown in Figure 25(c). When unloading, the internal force of the material is the difference between the elastic force and the viscous force, so the unloading curve bc is under the static load curve bo. When the loading and unloading speed is very large, the loading and unloading curves of visco-elastic materials do not coincide. The greater the material viscosity and the loading and unloading speed, the greater the difference between the two curves. When the unloading speed is very large, the elastic deformation is limited by the viscous internal resistance, so there is a part of elastic deformation, such as the oc section shown in Figure 25(c), and the cd segment in the Figure is an elastic deformation which can be recovered immediately at the unloading stage. There is no external force after unloading, so the elastic force of the material tries to recover the visco-elastic deformation at the end of the unloading stage. However, viscous resistance limits the recovery of material deformation, so the visco-elastic deformation cannot be restored immediately after unloading, but gradually disappears with time. This process is called visco-elastic recovery of materials. Due to the visco-elastic recovery, the stress and strain in Figure 25(c) are gradually returned to the origin 0 points from the c point after unloading. Thus, the stress-strain curve of the visco-elastic material becomes a closed curve, as shown in Figure 25(c) of oabco, and such a closed curve is called a viscous hysteretic curve. The area of the hysteresis curve is the amount of energy consumed by the viscous internal resistance of the unit volume of a material in a loading unloading cycle. (Chapman & Cowling 1970, Pp.125-128.)

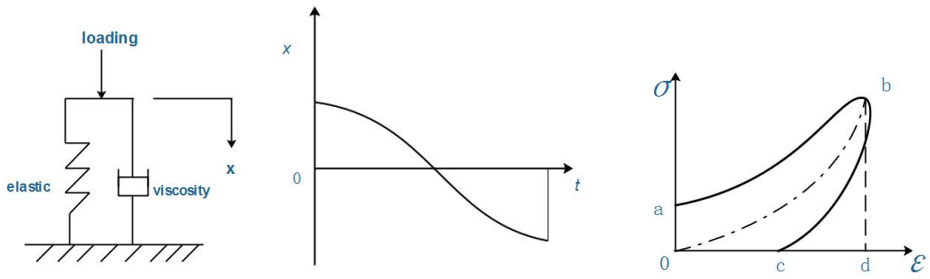

a b c

Figure 25. Stress-Strain Curve for Visco-elastic Material

3.1.4. Creep

Creep is a phenomenon that increases with time under certain static conditions. The cushioning package is always undergoing deformation during storage, so even before the creep falls from the same height, the acceleration produced by the built-in product is also different. Creep is directly related to load size. Figure 26 shows the relation between deformation and time under different loads. When the material gets force F2, it immediately produces an instantaneous deformation value of a, which has nothing to do with the loading time and is the representation of the general elasticity of materials. Then there is a process where creep rates change very rapidly but gradually decrease so that they remain constant over time. When the stress is large enough, there may be third stages, that is, from the steady development to the accelerated creep stage, the creep process is approximately represented as Figure 27.

Creep is not only related to load and time, but also to temperature and it increases obviously with the increase of temperature. Cushioning materials, such as foam plastics, have obvious creep even at room temperature. While the package needs to be stored for long term, which provides the conditions for creep of the packing material. Creep causes plastic deformation of the material and increases the gap between the liner and the product which can easily cause two shocks to the product. (Branson & Christiason 1971, Pp. 257-278.)

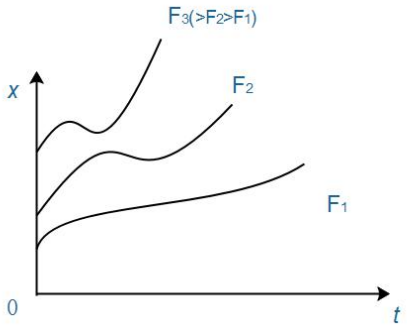

Figure 26. Creep Curve in Different Load

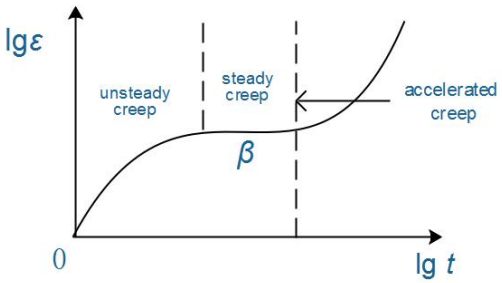

Figure 27. Typical Creep Curve for Packaging Material

After understanding the basic mechanical properties of cushioning materials, a detailed study of the drop impact response of nonlinear packages can be carried out.

3.2. Drop impact response analysis of nonlinear package

Nonlinear packages are the most common examples in practice, analyzing the drop impact response of them can provide more valuable suggestions when we design packaging for them.

3.2.1. Dynamic model of package

Impact is a very complex physical phenomenon. In order to analyze and calculate the response of packaging products to vibration and shock, the package is simplified as a dynamic model. As shown in Figure 28, the drop mechanical model for a single degree of freedom linear cushioning packaging system is presented. Suppose the outer packing container is homogeneous rigid body M, the packaged product is a homogeneous rigid body m, the cushioning material is linear elastic material, regardless of the quality of the cushioning material, k and c represent elastic coefficient and coefficient of viscous damping of cushion lining respectively.

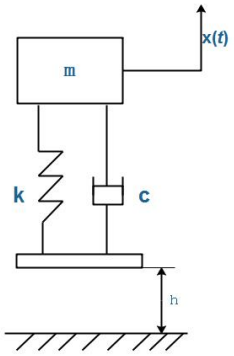

Figure 28. One freedom degree Cushion Packaging System Model

3.2.2. Mathematical model of liner pressure deformation

As mentioned earlier, there are two basic types of nonlinear packaging materials: One is hard elasticity, the other is soft elasticity, and the more complex nonlinear elastic material can be regarded as a combination of these two basic types. The mathematical model of liner pressure deformation is expressed as an approximate expression of the pressure deformation curve of the cushioning gasket. (Rouillard 2004, Pp.237-247.)

There are many forms of approximate expressions which can reflect the characteristics of a rigid elastic pad, in which the tangent equation and the cubic equation are often used. When the tangent equation is used as a mathematical model, the pressure deformation curve of the liner can be expressed as:

$$P = \frac{2k_0 d}{\pi} \tan \frac{\pi x}{2d} \tag{29}$$

In the equation, k_0 is the initial elastic constant of the gasket, which is the tangent slope of the liner pressure deformation curve at the origin; d is backing the limit deformation, which means that straight $x = d$ is a liner pressure deformation curve asymptotic.

While the cubic equation is used as the mathematical model, the pressure deformation curve of the liner can be expressed as:

$$P = k_0 x + r x^3 \tag{30}$$

In the equation, the k_0 is the initial elastic constant of the liner, and r is the nonlinear constant of the hard-elastic liner. r>0, whose unit is N/m^3. (Rouillard 2004, Pp.237-247.)

There are many forms of approximate expressions that reflect the characteristics of soft elastic cushions, among which the hyperbolic tangent equation and the cubic equation are often used. When the hyperbolic tangent equation is used as the mathematical model, the pressure deformation curve of the liner can be expressed as

$$P = P_0 th \frac{k_0 x}{P_0} \tag{31}$$

In the equation, the k_0 is the initial elastic constant of the liner, and the P_0 is the ultimate pressure that the gasket can bear. When the cubic equation is used as the mathematical model, the pressure deformation curve of the liner can be expressed as:

$$P = k_0 x - r x^3 \tag{32}$$

In the equation, the k_0 is the initial elastic constant of the liner, and r is the nonlinear constant of the soft elastic liner. r>0, whose unit is N/m^3. To change the equation (32) into a negative characteristic, P is required to be an increasing equation of x, that is,

$$\frac{dP}{dx} = k_0 - 3rx^2 > 0 \tag{33}$$

Therefore, the mathematical model of soft elastic pad with cubic equations is the following limit for the value of x:

$$x \le \sqrt{\frac{k_0}{3r}} \tag{34}$$

The pressure deformation relation of the liner is unique, but there are many forms of mathematical model that can describe this relation. The choice of mathematical model has both a certain degree of accuracy and the solution of the problem as simple as possible.

According to the above principle, the mathematical model of nonlinear elastic packing is usually taken as the cubic equation. (Edwards & Good 2001, Pp.215-225.)

In cushioning packaging design, the design can be based on Newton's second law. Based on establishing the mathematical model of cushion pressure deformation and the integral equation of shock response, the acceleration time equation of the product and the damaged parts under the nonlinear condition is solved by using elliptic integral method.

3.2.3. Integral solution of product response acceleration time equation

Integral equation for drop impact of package

Assuming that the cushion liner is a nonlinear elastic liner, the relationship between the deformation and the pressure is:

$$P = P(x) \tag{35}$$

The package falls at a height of H, taking the natural thickness of the cushion as the basis and taking the X axis downward and neglecting the weight and the cushion damping, the differential equation of motion after the landing of the product as shown in Figure 29 is:

$$\ddot{x} = -\frac{1}{m}P(x) \tag{36}$$

Using $2\dot{x}$ to multiply both side, the equation can be given

$$2\dot{x}\ddot{x} = -\frac{2\dot{x}}{m}P(x) \tag{37}$$

So the upper left side can be rewritten as:

$$2\dot{x}\ddot{x} = 2\dot{x}\frac{d\dot{x}}{dt} = \frac{d}{dt}(\dot{x^2}) \tag{38}$$

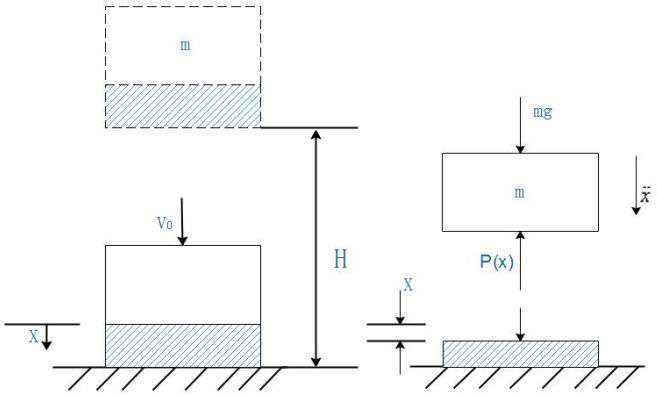

Figure 29. Chart of Packaging Dropping Process

Take it back into equation (38):

$$d(\dot{x}^2) = -\frac{2}{m}P(x)dx \tag{39}$$

When the package falls to the floor, $t = 0, x = 0$. The corresponding

$$\int_{\sqrt{2gH}}^{\dot{x}} d(\dot{x}^2) = -\frac{2}{m}\int_0^x P(x)dx \tag{40}$$

interval is integral to the differential equation above, so

$$x^2 = 2gH - \frac{2}{m}\int_0^x P(x)dx \tag{41}$$

Square the upper sides of the upper equation,

$$\dot{x} = \frac{dx}{dt} = \sqrt{2gH - \frac{2}{m}\int_0^x P(x)dx} \tag{42}$$

Separating the upper variables and accumulating the corresponding interval, it can be given:

$$t = \int_0^x \frac{dx}{\sqrt{2gH - \frac{2}{m}\int_0^x P(x)dx}} \tag{43}$$

Equation (43) is an integral equation, whose solution represents the functional relationship between the displacement and time when the product is impacted. (Wong & Mai 2006, Pp.930-938.)

A:Drop shock response of hard elastic packages

1) Maximum displacement of the product

The cubic equation relation of pressure and deformation of the liner is:

$$P = k_0 x + r x^3 \tag{44}$$

Putting the upper equation in to equation (42):

$$\dot{x^2} = 2gH - \frac{2}{m}\int_0^x (k_0 x + r x^3) dx \tag{45}$$

$$= \frac{r}{2m}\left(\frac{4WH}{r} - \frac{2k_0}{r}x^2 - x^4\right)$$

In the equation, W=mg, it is the gravity of the content product, because the equation:

$$x^4 + \frac{2k_0}{r}x^2 - \frac{4WH}{r} = 0 \tag{46}$$

And the root of the above equation

$$x^2 = -\frac{k_0}{r} \pm \sqrt{\frac{k_0^2}{r^2} + \frac{4WH}{r}} \tag{47}$$

So, we let

$$\left.\begin{matrix} a^2 \\ b^2 \end{matrix}\right\} = \sqrt{\frac{k_0^2}{r^2} + \frac{4WH}{r}} \pm \frac{k_0}{r} \tag{48}$$

So, the original equation can be decomposed into

$$\dot{x^2} = \frac{r}{2m}(a^2 + x^2)(b^2 - x^2) \tag{49}$$

The above equation shows that the main real condition is $x \le b$. (Wang & Lu 2005, Pp.667-680.) Therefore, when the package falls, the maximum displacement of the product is

$$x_m = b = \sqrt{\frac{1}{r}\left(\sqrt{k_0^2 + 4rWH} - k_0\right)} \tag{50}$$

2) Application of elliptic integral

According to equation (49), the integral equation for solving the problem of hard elastic drop impact is

$$t=\sqrt{\frac{2m}{r}}\int_0^x \frac{dx}{\sqrt{\left(a^2+b^2\right)\left(b^2-x^2\right)}} \tag{51}$$

In order to facilitate the application of elliptic integral tables, calculations are made

$$x=b\cos\varphi=x_m\cos\varphi \tag{52}$$

In order to facilitate the application of elliptic integral tables, calculations are made

$$e^2=\frac{b^2}{a^2+b^2} \tag{53}$$

Because

$$a^2+b^2=a\sqrt{\frac{k_0^2}{r^2}+\frac{4WH}{r}} \tag{54}$$

$$=2\left[\frac{1}{r}\left(\sqrt{k_0^2+4rWH}-k_0\right)+\frac{k_0}{r}\right]=\frac{2}{r}\left(rx_m^2+k_0\right)$$

And

$$b=x_m \tag{55}$$

So

$$e^2=\frac{rx_m^2}{2\left(k_0+rx_m^2\right)} \tag{56}$$

And

$$dx=-b\sin\varphi d\varphi=-x_m\sin\varphi d\varphi \tag{57}$$

$$=\frac{2}{r}\left(k_0+rx_m^2\right)\left(1-e^2\sin^2\varphi\right)$$

$$b^2-x^2=b^2\left(1-\cos^2\varphi\right)=x_m^2\sin^2\varphi \tag{58}$$

When $x=0$, $\varphi=\frac{2}{\pi}$. Substituting the above three types into equation (51):

$$t=\sqrt{\frac{m}{k_0+rx_m^2}}\int_{\frac{\pi}{2}}^{\varphi}\frac{-d\varphi}{\sqrt{1-e^2\sin^2\varphi}} \tag{59}$$

$$t=\sqrt{\frac{m}{k_0+rx_m^2}}\left[\int_0^{\frac{\pi}{2}}\frac{-d\varphi}{\sqrt{1-e^2\sin^2\varphi}}-\int_0^{\varphi}\frac{-d\varphi}{\sqrt{1-e^2\sin^2\varphi}}\right] \tag{60}$$

$F(e)$ and $F(e,\varphi)$ are used to represent the two definite integrals in the upper equation

$$F(e)=F\left(e,\frac{\pi}{2}\right)=\int_0^{\frac{\pi}{2}}\frac{d\varphi}{\sqrt{1-e^2\sin^2\varphi}} \tag{61}$$

$$F(e,\varphi)=\int_0^{\varphi}\frac{d\varphi}{\sqrt{1-e^2\sin^2\varphi}},\ F(e,\varphi)=\int_0^{\varphi}\frac{d\varphi}{\sqrt{1-e^2\sin^2\varphi}} \tag{62}$$

$F(e)=F(e,90^\circ)$ is called the first kind of complete elliptic integral, and $F(e,\varphi)$ is called the first kind of incomplete elliptic integral. Replace the equation (61) and (62) into (60).

$$t=\sqrt{\frac{2m}{2k_0-rx_m^2}}\int_0^{\varphi}\frac{d\varphi}{\sqrt{1-e^2\sin^2\varphi}}=\sqrt{\frac{2m}{2k_0-rx_m^2}}F(e,\varphi) \tag{63}$$

3) Parametric equation of product displacement time curve

Combining the equation (63) and equation (60), the parameter equation of the product displacement time curve is obtained:

$$\left.\begin{aligned}x&=x_m\cos\varphi\\ t&=\sqrt{\frac{m}{k_0+rx_m^2}}\left[F(e)-F(e,\varphi)\right]\end{aligned}\right\} \tag{64}$$

When $x=x_m$, $\varphi=0$, $F(e,\varphi)=0$. Therefore, the maximum value of instantaneous displacement of the product is

$$t_m=F(e)\sqrt{\frac{m}{k_0+rx_m^2}} \tag{65}$$

If the cushioning gasket is an ideal elastic liner, whose unloading curve coincides with the loading curve, and the x-t curve is symmetrical to the straight line $t = t_m$ so the impact time of the built-in product is

$$\tau = 2t_m = F(e)\sqrt{\frac{4m}{k_0 + rx_m^2}} \tag{66}$$

Putting (66) into (65), the parameter equation of product displacement time curve can be expressed as

$$\left.\begin{aligned} x &= x_m \cos\varphi \\ t &= t_m\left[1 - \frac{F(e,\varphi)}{F(e)}\right] \end{aligned}\right\} \tag{67}$$

$$\left[e = \sqrt{\frac{rx_m^2}{2\left(k_0 + rx_m^2\right)}}, \varphi = \frac{\pi}{2} \sim 0\right] \tag{68}$$

$$\ddot{x} = -\left(\frac{k_0}{m}x + \frac{r}{m}x^3\right) \tag{69}$$

In the equation (69), when $x = x_m$, The maximum acceleration response of the product can be obtained. (Wong & Mai 2006, Pp.930-938.)

B: Drop impact response of soft elastic packages

1) Maximum displacement of the product

Pressure deformation relation of cubic equation of gasket is

$$P = k_0 x - rx^3 \tag{70}$$

Substituting the above equation into equation (47), it can be obtained

$$P = k_0 x - rx^3 \tag{71}$$

$$\dot{x}^2 = 2gH - \frac{2}{m}\int_0^x (k_0 x - rx^3)dx \tag{72}$$

$$= \frac{r}{2m}\left(x^4 - \frac{2k_0}{r}x^2 + \frac{4WH}{r}\right) = \frac{r}{2m}\left(x^2 - a^2\right)\left(x^2 - b^2\right) \tag{73}$$

In the above formulate, a^2 and b^2 are the two roots of the below equation.

$$x^4 - \frac{2k_0}{r}x^2 + \frac{4WH}{r} = 0 \tag{74}$$

So

$$\left.\begin{matrix} a^2 \\ b^2 \end{matrix}\right\} = \frac{k_0}{r} \pm \sqrt{\frac{k_0^2}{r^2} - \frac{4WH}{r}} \tag{75}$$

Thus, the speed at which the product falls can be expressed as

$$\dot{x} = \frac{dx}{dt} = \sqrt{\frac{r}{2m}(x^2 - a^2)\left(x^2 - b^2\right)} \tag{76}$$

Because of $a^2 > b^2$, so $\dot{x}$ is real conditions for $x \le b$, the maximum displacement of package drop impact products is

$$x_m = b = \sqrt{\frac{1}{r}\left(k_0 - \sqrt{k_0^2 - 4rWH}\right)} \tag{77}$$

2) Application of elliptic integral

According to the equation (43), the integral equation for solving the product displacement time equation is

$$t = \sqrt{\frac{2m}{r}}\int_0^x \frac{dx}{\sqrt{\left(x^2 - a^2\right)\left(x^2 - b^2\right)}} \tag{78}$$

In order to apply the elliptic integral table, so

$$x = b\sin\varphi = x_m \sin\varphi \tag{79}$$

$$e^2 = \frac{b^2}{a^2} = \frac{rx_m^2}{2k_0 - rx_m^2} \tag{80}$$

So

$$dx = x_m \cos\varphi d\varphi \tag{81}$$

$$x^2 - a^2 = -\frac{1}{r}\left(2k_0 - x_m^2\right)\left(1 - e^2\sin^2\varphi\right) \tag{82}$$

$$x^2 - b^2 = -x_m^2\cos^2\varphi \tag{83}$$

Note, when $x = 0$, $\varphi = 0$. Substituting above three types into (75) can be obtained

$$t=\sqrt{\frac{2m}{2k_0-rx_m^2}}\int_0^{\varphi}\frac{d\varphi}{\sqrt{1-e^2\sin^2\varphi}}=\sqrt{\frac{2m}{2k_0-rx_m^2}}F\left(e,\varphi\right) \tag{84}$$

3) Parametric equation of product displacement time curve

The equation of the product displacement time curve is obtained by combining the equation (52) and (55)

$$\left.\begin{aligned} x&=x_m\sin\varphi\\ t&=\sqrt{\frac{2m}{2k_0-rx_m^2}}F(e,\varphi)\end{aligned}\right\} \tag{85}$$

When $\varphi=\frac{\pi}{2}$, $x=x_m$, the corresponding instantaneous is

$$t_m=F\left(e\right)\sqrt{\frac{2m}{2k_0-rx_m^2}} \tag{86}$$

Substituting the equation (65) into (64), the parameter equation of the product displacement time curve can be expressed as

$$\left.\begin{aligned} x&=x_m\sin\varphi\\ t&=t_m\frac{F(e,\varphi)}{F\left(e\right)}\end{aligned}\right\} \tag{87}$$

The shock duration of the product is

$$\tau=2t_m=F\left(e\right)\sqrt{\frac{8m}{2k_0-rx_m^2}} \tag{88}$$

Given product displacement, the acceleration of the product can be obtained

$$\ddot{x}=-\frac{1}{m}(k_0x-rx^3) \tag{89}$$

In the equation (66), the maximum acceleration response of the product can be obtained by making $x=x_m$. As can be seen above, when the package falls, the stress condition is related to the drop height and the elastic coefficient of the liner. In order to judge whether the package is damaged or not, it is necessary to discuss the product fragility or its damage boundary curve. (Wang & Lu 2005, Pp.667-680.).

3.3. Design rationality evaluation of nonlinear cushioning package

The maximum acceleration capability and can withstand the impact of product value and withstand the maximum acceleration value of the products of the anti-shock strength increases. We call the maximum acceleration that the product can sustain is the product's fragility, expressed in G_m . However, the single factor of maximum acceleration cannot fully express the impact strength of the product. However, the experimental tests show that for the same product, the maximum acceleration can be different if the pulse duration is different. In addition, when the velocity increment in the impact process Δv below a critical value Δv_c , even if the product has undergone the greatest acceleration, exceeding the original brittleness of the product, there is no breakage. Therefore, the concept of impact damage boundary curve is proposed, which fully reflects the relationship between acceleration peak value, speed variation, pulse waveform and product damage, and more perfectly demonstrates the ability of product shock resistance. The impact damage boundary curve is plotted at the peak of acceleration as ordinate and the velocity change is in abscissa in a two-dimensional coordinate system, which is the boundary between the damaged area and the safety zone. When the package falls shock, the product has a certain and Δv . Therefore, there is a corresponding certain point in the Gm coordinate system $G_m - \Delta v$. If this point falls within the damaged area of the product's damaged boundary curve or on the damaged boundary, the product will be damaged, otherwise it will not be damaged. Therefore, the integral method is used to obtain the maximum acceleration response and the duration of shock. We can combine the broken boundary curve of the product and make use of the above principle to judge the design rationality of the packing material of the cushioning material.

Above, we discuss the method of solving drop impact response of nonlinear package by using elliptic integral. Although the cushioning properties of the material depend mainly on the compressive stress and bending stress of the material itself, but in the case of high

velocity impact, the damping property of the material will influence the cushioning performance of the liner material, and in a certain range of ratio, the material can reduce the peak acceleration when the product shocks. Therefore, the calculation results do not take into account the influence of material damping characteristics on the performance of the cushion, and the maximum acceleration value is greater than the actual value, so it needs to be corrected properly. However, the damping of the material has little influence on the impact time, and the integral method can be used to estimate the time and waveform of the drop impact of the package. (Lu, Tao & Gao 2013, Pp.32-42.) In addition, this method can compare the performance of cushioning packaging materials on the other hand from the material cushioning characteristics. Therefore, the theoretical analysis of the drop impact of the nonlinear package can provide a basis for the selection of cushioning packaging materials.

We should also see that, in practice, the force and deformation curves of many materials can be described by cubic equations. But some materials, such as molded pulp products, are buffered by their structural deformation. Therefore, the above equation is not applicable to all cushioning packaging materials.

3.4. Conclusions

In this chapter, the influence of plasticity and viscosity of the material on the cushioning performance of the material is introduced according to the stress-strain curve. On the establishing the mechanical model of cushion and the integral equation of shock response, the method of solving the acceleration time equation of packing under nonlinear condition is put forward. Then, the concept of product impact fragility and product damage boundary curve is introduced, and the method of theoretical evaluation of cushioning package design is discussed. Finally, the practical significance and limitations of the theoretical calculation method for the drop impact response of nonlinear package are further analyzed.

4. STUDY ON SIMULATION METHOD OF CUSHIONING PACKAGING

For the cushioning packaging of products, most of them are designed by cushioning characteristic curve of cushion materials. Although the cushioning characteristic curve of the material is the experimental curve, the imperfection of testing technology and the neglect of structural factors make it impossible to design cushioning packaging accurately. Therefore, to investigate whether the package meets the requirements, the designed prototype package is subjected to drop impact tests in accordance with the specified environmental conditions. If the package does not meet the requirements, we need to modify the design, reproduce the prototype packaging and test again until the qualified. (Dominic 2005, Pp.151-160.)

The drop test of cushion package requires destructive test of the sample, the test cycle is long, the cost is great, and the course of the test is short. So, it is difficult to observe the test process phenomena, and the collision boundary conditions (such as drop angle, etc.) of the drop test are difficult to control, and it is also impossible to measure the characteristics of vulnerable parts in the test. Computer modeling is used to simulate the drop impact process of package, and only a package finite element model is established. The computer can do a variety of angles and height drop analysis, the simulation results include all the dynamic process information of almost any location of the whole model, which can visually and dynamically demonstrate the change of various physical quantities during the whole drop process. Moreover, simulation analysis can be carried out in the packaging design stage. The analysis results can provide guidance for the modification of cushioning packaging design and reduce the test cost and optimize the packaging design.

This chapter mainly studies the cushioning packaging system using expanded polyethylene as gasket. The finite element theory and ANSYS / LS-DYNA are applied to analyze dynamic response of the product fall process (Wang 2005, Pp. 667-680.). It provides a new method for designing reasonable cushioning package and increasing the speed of product research & development, which can supplement and perfect the traditional design system of cushioning transportation packaging.

4.1. Scheme design of simulation for buffer packaging

The drop impact test in laboratory is a test of resistance to vertical impact in the process of circulation of goods (packages). The numerical simulation analysis of cushion packaging is to use simulation software to simulate the drop test of package, to analyze and evaluate the cushioning effect of cushioning transportation package.

4.1.1. Standard introduction of dropping test

Drop test method for transport package of GB/T 4857.5 standard specifies the drop impact test method for packages. The drop tests are applied to simulate the fall of transport packages with free fall which is suitable for smaller transport packages. According to Chinese national standards and international standards, the quality of the transport package for free fall test is generally less than 100kg. For the transport packages beyond the quality range, the rotating drop test should be used.

The free fall test can be divided into three different forms: surface drop, edge drop and angle drop. When the surface falls, the falling surface of the sample is parallel to the impact surface, and the maximum angle is not more than 2°; When the edge falls, the gravity line of the sample is made up of the falling edge, and the angle between one plane of the two edges of the sample and the angle of the impact surface is not more than ±5°, or 10% of the included angle; The drop is parallel to the horizontal plane, with an angle of no more than 2°; When the angle drops, the gravity line of the sample passes through the

falling angle, and the error of the angle of at least two planes constituting the angle of the sample and the impact surface shall be no more than ±5° or 10% of the included angle.

4.1.2. Program development of numerical simulation of cushioning packaging

1) **Fundamentals of dynamic software analysis**

The LS-DYNA program is a fully functional geometric non-linearity (large displacement, large rotation and large strain), material non-linearity (more than 140 material dynamics models) and contact non-linearity (more than 50) procedures (Sek 2000, Pp. 249-255.). The algorithm is based on explicit solution and has implicit solution equation. With nonlinear dynamic analysis as the main part, it has both static analysis equation (such as pre-stress calculation before dynamic analysis and spring-back calculation after sheet metal forming); It is a general structural analysis nonlinear finite element program combined with military and civil use.

There are two kinds of finite element calculation methods: implicit solution and explicit solution. (Saeed 2008, Pp.144-147.)

The governing equations of a dynamic system is shown as below:

$$M\ddot{x} + C\dot{x} + Kx = F \tag{90}$$

x is nodal displacement, M, C and K represent mass matrix, damping matrix and stiffness matrix respectively. (Saeed 2008, Pp.144-147.)

By integrating the time step, the system state of the *t*+*dt* moment can be predicted under the condition of the known *t* moment system. That is, if the explicit solution is used, the equation (90) can be written

$$M\ddot{x}_{t+dt} = F - C\dot{x}_t - Kx_t \tag{91}$$

If F_{t-dt} , x_{t-dt} is the known initial condition, then the substitute equation (88) can find and according to

$$\dot{x}_{t+dt} = \dot{x}_t + \ddot{x}_t dt \tag{92}$$

$$x_{t+dt} = x_t + \dot{x}dt + \frac{1}{2}\ddot{x}_t(dt)^2 \tag{93}$$

So we can obtain the velocity, displacement, and substitute (91), we can get the acceleration x_{t+dt} and so on. If implicit solution is used, equations must be used

$$M\ddot{x}_t + C\dot{x}_t + Kx_t = F_t \tag{94}$$

The velocity displacement x_t and acceleration are unknown quantities, then the differential equation of the matrix must be solved to obtain the result. If the equation is complex and involves nonlinear problems, and sometimes it cannot find the solution which can satisfy the requirement.

It is obvious that the solution equation (91) is much simpler than the equation (94) in the individual time step. The explicit solution (94) does not require matrix transformations, and the computational complexity is also small; Moreover, when the material non-linearity and geometric non-linearity need to be considered, the explicit solution will not increase the computational complexity, which is just not the implicit solution.

However, explicit solutions are not recommended for solving static problems, because the fatal weakness of this method is the lack of stability. When the time division is too large, the calculation error will be very large, and even the convergent solution cannot be found. Therefore, it is necessary to find enough small-time steps to meet the requirements of computational accuracy. So that for simple static problems, it cannot reflect its superiority, but it is less convenient than implicit solution. Based on the above reasons, the ANSYS/LS-DYNA module using explicit solution is an effective tool for analyzing drop impact problems. (Saeed 2008, Pp.144-147.)

2) Application of ANSYS/LS-DYNA in drop response analysis of package

The mechanical behavior of cushion packaging belongs to transient, large deformation and nonlinear behavior. In general, simple finite element software cannot solve transient, large deformation, nonlinear behavior. If the software does not contain material model for packaging materials, it cannot accurately predict the behavior of packaging materials. ANSYS/LS-DYNA software can not only solve transient, large deformation and nonlinear mechanical problems, but also contains more than a dozen packaging material models. It is the software that provides the most packaging model in all the finite element analysis software (Sahoo 2007, p.4245.). Users can choose the appropriate material model for simulation analysis according to the type of product packaging materials. ANSYS/LS-DYNA software can simulate a variety of cushioning packaging materials, including EPE, EPS, EPU and various types of paper, etc.

Additional program module for drop test, Drop Test Module(DTM), is provided in ANSYS/LS-DYNA. The module is specially developed for drop analysis and can easily set up the parameters of gravity acceleration, drop height, drop angle, solution time, output data, output steps, initial velocity and ground properties, with simulating different drop positions and angles for drop simulation analysis of product cushioning packaging model. Using ANSYS/LS-DYNA post-processing program can show the products of different parts in the process of drop impact deformation and stress state of different time, the overall energy changes, and the cushion on the absorption of energy, and shows the failure mechanism of the product, providing the basis for the structural design and improvement of packaging design. (Rust & Schweizerhof 2003, Pp.227-244.)

4.2. Establishment of LCD (liquid crystal display) package model

To simulate the simulation as accurately as possible, it is necessary to understand the structure and size of the LCD display package accurately with the modeling software, especially the internal structure of LCD.

4.2.1. LCD package prototype

Understanding the connection patterns and structures allows for reasonable simplification. From the complete LCD display package to the LCD display, disassemble to the LCD screen and steel frame, as shown in Figure 30 to Figure 35.

Figure 30. Integral package of LCD

Figure 31. Back of LCD

Figure 32. Front of LCD

Figure 33 Profile of LCD

Figure 34. Front shell of LCD

Figure 35. Back shell of LCD

4.2.2. Establishment of geometry model

ANSYS Workbench can be seamlessly connected with modeling software, so you can model it with your own familiar modeling software. It is the Solidworks software with the connection of ANSYS. It will appear "ANSYS" option on “menu bar” of Solidworks after the connection. So, the "Workbench" option can be started. At the same time, the model is called by Workbench. The model was built in Solidworks, and Workbench was opened under the software. The model was automatically imported into Workbench, so the model of LCD package was constructed in Solidworks.

The geometric modeling of liquid crystal display package using Solidworks is the first step in the simulation of package performance. The proper geometry model not only makes the pre-processing process easy to complete, but also helps to reduce the computation time and obtain the ideal simulation results; If the geometric model is not appropriate, it is difficult to obtain credible simulation results, and even cannot complete the normal simulation.

Understanding the structure and assembly relation of each part of LCD package, we can make geometric modeling. The geometric model is a combination of geometric elements which are approximately the same as the actual structure, and the same degree depends on the accuracy of the calculation and the principle of structural simplification. And when the same product has different types of simulation analysis, the geometric models used in each

analysis are not the same. Therefore, the establishment of geometric model not only depends on the reality of the product, but also consider the types and characteristics of the following simulation analysis. The purpose of the simulation is to select the important parameters in the model to make it close to reality. According to the research contents, this paper carried out detailed modeling for packaging liquid crystal display package and buffer foam, the LCD and shell before and after steel structure was simplified.

Figure 36 is the geometry model of LCD assembly with the package. When assembling the packages, to facilitate the analysis of the amount of deformation of the simulation results, the center of the package is selected on the LCD screen, and the assembly of the center of the LCD screen coincides with the origin point. Figure 37 and Figure 38 are the screen of LCD and the cushion foam.

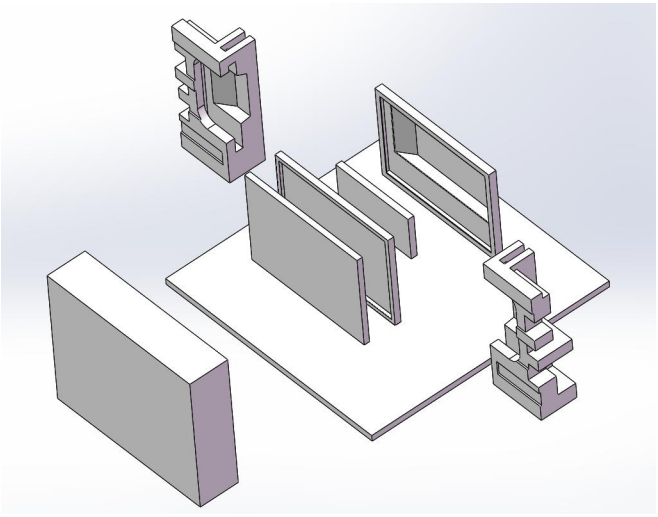

Figure 36. Geometry model of LCD assembly with the package

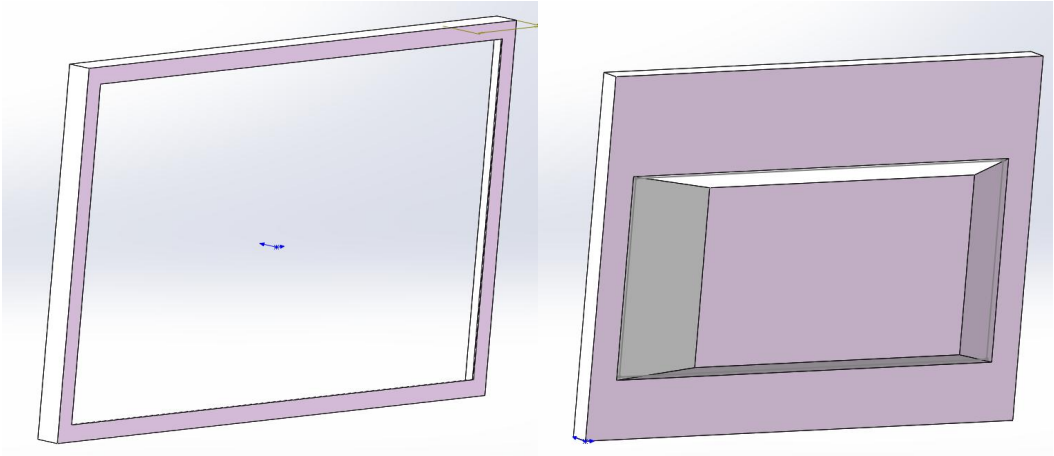

Figure 37. The front and the back side of the LCD

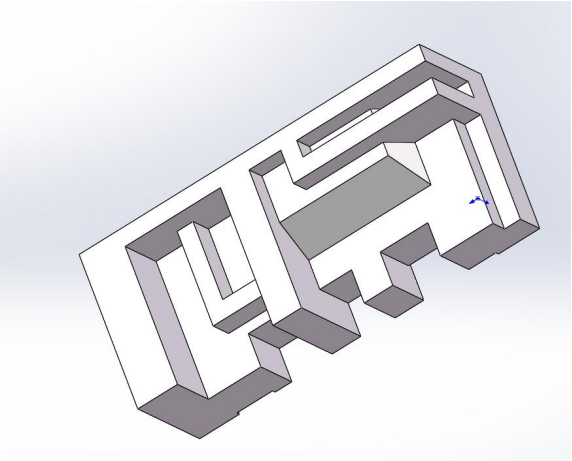

Figure 38. Cushion foam

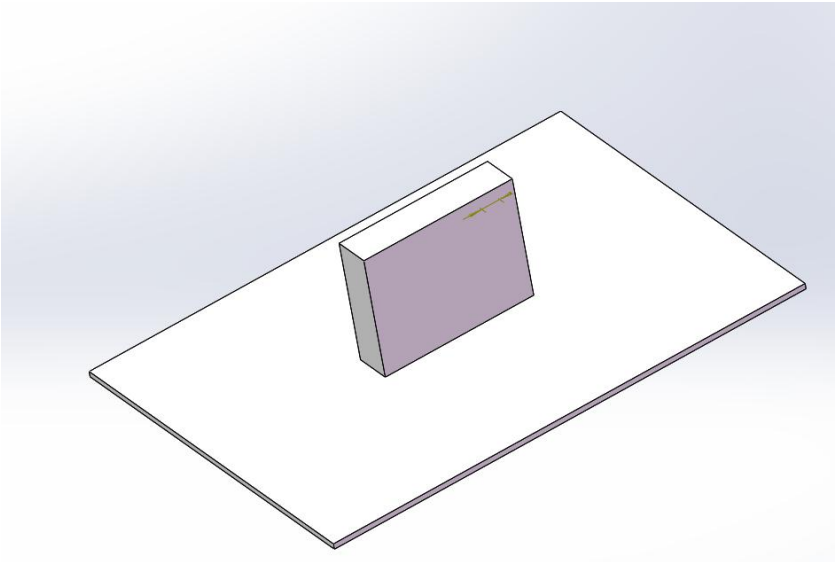

Figure 39. Final assembly structure

After building the LCD package model, we also need to build a drop board. According to the second chapter, the size of the drop board is 1700mm× 1260mm×20mm (L×W×H). As shown in Figure 39, the drop test machine falls board geometry model. Newtonian mechanics in package drop in the application of the known package height can be calculated to fall in packages at critical state speed. In order to save computing time, in the fall simulation, the velocity value can be assigned to the package, eliminating the fall process of the package; Through previous experiments, we can find that, in a given package drop speed, if the model in the package and the falling board is in direct contact with the situation, then the simulation results are inconsistent with the actual situation. Because it is equivalent to a package of pressure, its speed will always decrease to zero, the package will not rebound. If the package and the falling board is arranged between a certain distance, it can reflect the real situation falls, so this paper set up the package and drop plate distance is 2mm.

4.3. Material parameter setting

The definition of material model is a very important link in numerical simulation, and it directly affects the accuracy and reliability of numerical simulation. In general, the following points should be noted in defining a material model:

1) For each cell type, it is not possible to use all the material models. For example, in this topic, the package does not use shell units, because shell elements cannot use anisotropic material models. Therefore, refer to the cell manual, you need to determine the model you can use when you start to use it.
2) Not all the parameters of the material model should be defined.
3) When defining material properties, make sure that a consistent unit system is used. The incorrect system of units will not only affect the material response, but also affect the calculation of contact stiffness.
4) The choice of material model depends on the material to be analyzed and the material parameters that can be obtained.

5) Don't underestimate the importance of accurate material data to the results and try to spend extra effort getting accurate material data.

Workbench comes with some commonly used materials that need to be defined due to different simulation analyses. For example, the bilinear kinematic hardening model (BKIN: Bilinear Kinematic Hardening Plasticity) is only suitable for small strain situations. If the strain is large, we should consider the bilinear hardening model. Otherwise, the operation is prone to error or the problem of negative volume, so we can define for the specific problem.

The model is fully simplified. In this paper, a package display includes two EPS cushioning foam, plastic shell, steel, LCD screen, and simplified circuit board mass (including fixed steel frame) and the outer package and drop plate. So, it is needed to define the material for these six parts. The material of drop board is made of steel, the parameters are shown in Figure 40.

Properties of Outline Row 9: Structural Steel

	A	B	C	D	E
1	Property	Value	Unit		
2	Density	7850	kg m^-3		
3	Isotropic Elasticity				
4	Derive from	Young's Modulu...			
5	Young's Modulus	2E+11	Pa		
6	Poisson's Ratio	0.3			
7	Bulk Modulus	1.6667E+11	Pa		
8	Shear Modulus	7.6923E+10	Pa		
9	Specific Heat	434	J kg^-1 C^-1		

Figure 40. Material parameter of drop board

The material parameter of LCD is related to the glass. The density of the glass is $2500\,kg/m^3$. The thickness of the LCD screen is $20mm$, leading to the weight of the screed is more than $5kg$. Maximum deformation can reach to $30mm$ at $8ms$ when the density is $2500\,kg/m^3$. To lighten the weight of the package, the density is changed into $250\,kg/m^3$,

so that the maximum deformation can reach to 15*mm* at 6*ms*. It can be seen that the quality has a great influence on the spring-back of the package, but the maximum acceleration of the simulation results is about $10^4 \sim 10^5$. The parameters is as shown in Figure 41. (Porras-Hurtado, Ruiz, Santos, Phillips, Carracedo & Lareu 2013. p.98)

Properties of Outline Row 8: LCD

	A	B	C	D	E
1	Property	Value	Unit		
2	Density	250	kg m^-3		
3	Isotropic Elasticity				
4	Derive from	Young's Modulu...			
5	Young's Modulus	6E+10	Pa		
6	Poisson's Ratio	0.25			
7	Bulk Modulus	4E+10	Pa		
8	Shear Modulus	2.4E+10	Pa		

Figure 41. Material parameter of LCD

The material of cushion foam is EPS. The density is $12E-08kg/mm^3$. The modulus of elasticity is $3.0Mpa$. The parameters is as shown in Figure 42.

Properties of Outline Row 7: EPS

	A	B	C	D	E
1	Property	Value	Unit		
2	Density	12	kg m^-3		
3	Isotropic Elasticity				
4	Derive from	Young's Modulu...			
5	Young's Modulus	1.5E+06	Pa		
6	Poisson's Ratio	0.1			
7	Bulk Modulus	6.25E+05	Pa		
8	Shear Modulus	6.8182E+05	Pa		

Figure 42. Material parameter of EPS

The outer packing box is made of tile board, its parameters is as shown in Figure 43.

Properties of Outline Row 6: corrugated box

	A	B	C	D
1	Property	Value	Unit	
2	Density	189	kg m^-3	
3	Isotropic Elasticity			
4	Derive from	Young's Modulu...		
5	Young's Modulus	7.38E+08	Pa	
6	Poisson's Ratio	0.32		
7	Bulk Modulus	6.8333E+08	Pa	
8	Shear Modulus	2.7955E+08	Pa	

Figure 43. Material parameter of the tile board

The material parameter of PCB mass block is as shown in Figure 44.

Properties of Outline Row 5: circut board

	A	B	C	D	E
1	Property	Value	Unit		
2	Density	1900	kg m^-3		
3	Isotropic Elasticity				
4	Derive from	Young's Modulu...			
5	Young's Modulus	2.21E+09	Pa		
6	Poisson's Ratio	0.3			
7	Bulk Modulus	1.8417E+09	Pa		
8	Shear Modulus	8.5E+08	Pa		

Figure 44. Material parameter of PCB mass block

Inner steel frame is choosing aluminum alloy material from the material library as shown in Figure 45.

Properties of Outline Row 4: alloy

	A	B	C	D	E
1	Property	Value	Unit		
2	Density	2770	kg m^-3		
3	Isotropic Elasticity				
4	Derive from	Young's Modulu...			
5	Young's Modulus	7E+09	Pa		
6	Poisson's Ratio	0.3			
7	Bulk Modulus	5.8333E+09	Pa		
8	Shear Modulus	2.6923E+09	Pa		
9	Bilinear Isotropic Hardening				
10	Yield Strength	2.9E+08	Pa		
11	Tangent Modulus	5E+08	Pa		

Figure 45. Material parameter of Inner steel frame

The shell is using composed material as shown in Figure 46

Properties of Outline Row 3: ABS/PC

	A	B	C	D	E
1	Property	Value	Unit		
2	Density	1070	kg m^-3		
3	Isotropic Elasticity				
4	Derive from	Young's Modulu...			
5	Young's Modulus	2.35E+09	Pa		
6	Poisson's Ratio	0.3879			
7	Bulk Modulus	3.4939E+09	Pa		
8	Shear Modulus	8.466E+08	Pa		
9	Bilinear Isotropic Hardening				
10	Yield Strength	4E+07	Pa		
11	Tangent Modulus	8.5E+08	Pa		

Figure 46. Material parameter of shell

4.4. Model checking and editing

Export *k* document from the explicit dynamics in workbench. Because the circuit board and the inner steel frame are tightly fixed together, these two parts will form a new part. When painting the mesh, the system will default that the two part is at together, and they will also share the nodes, as shown in Figure 47.

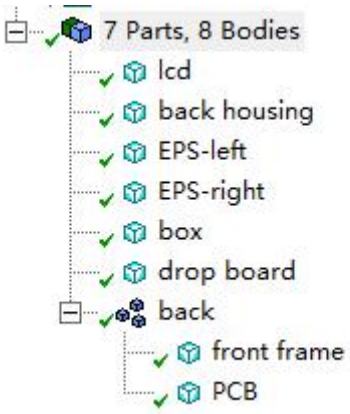

Figure 47. Geometric model tree of LCD package

4.5. Contact setting of each part of package

4.5.1. Main contact theory and contact type

Contact problem is a highly nonlinear behavior, usually referred to as contact when the two independent surfaces contact each other and are tangent. More computational resources are needed for the analysis of contact problems. The characteristic of contact is the

non-linearity of state change the system stiffness depends on the state of contact, that is, contact or separation between components. For the body, its density is only needed for the calculation of material properties, quality and other material properties will be ignored, in parts of the center will automatically be defined as internal coordinates, because it is rigid and does not need to calculate the stress, strain and relative deformation, thus eliminating the need for a mesh. In the interior processing, the rigid body is expressed as the point mass in the center of the inertial coordinate system. So, a rigid flexible body contact means to contact area in one or several parts as rigid body almost no deformation, when the general material and hard material soft contact, can be attributed to such problems.

In Workbench, five different types of contacts are provided: Bonded, No-Separation, Rough, Friction-less and Frictional, their characteristics are described in Table 4. In these five types, only Bonded, No-Separation two approach is linear, the calculation only need one iteration, the other three are nonlinear contact method, and need more iteration times. Note that No-Separation and Rough contact type do not apply to display dynamic analysis, if you set this contact relationship, it will display a warning message in the column: the constraint is ignored. (Porras-Hurtado, et al 2013, p.98)

Table 4 Characteristics of different contact types

Contact Types	Iteration times	Normal segregation	Tangential slip
Bonded	Once	Gap-less	Not allowed
No Separation	Once	Gap-less	Allowed
Rough	Many times	Allow clearance	Allowed
Friction-less	Many times	Allow clearance	Not allowed
Frictional	Many times	Allow clearance	Allowed

In the workbench, the contact algorithm is Pure Penalty, but in friction-less or frictional contact of large deformation problem, Augmented Lagrange is utilized. As fir Bonded

contact, Pure Penalty equation and General stiffness used in Mechanical. Because the high contact stiffness can have realized small or negligible penetration, and accurate results can be obtained. For friction-less or frictional contacts, Augmented Lagrange or Normal Lagrange are used, usually using Augmented Lagrange. In the contact setting, the contact surface and the target surface are also very important, the contact surface is red, and the target surface is blue. If the contact surface and the target surface are reversed, the contact pair can be hit right and modified by "Flip Contact/Target". Contact surface selection should pay attention to the following points:

(1) If a convex surface is to be in contact with the plane or the four sides, the plane or concave surface should be selected as the target surface;

(2) If a surface has a rough mesh and another surface mesh is fine, the rough mesh surface should be chosen as the target surface;

(3) If one surface is harder than the other, the hard surface should be chosen as the target surface;

(4) If one surface is high order and the other surface is low order, the lower surface should be the target surface;

(5) If the surface is larger than the other surface, the large surface should be the target surface. (Sahoo & Ghosh 2007, p.4245).

4.5.2. Contact setting of package drop simulation

Workbench can automatically detect and establish mutual contact between components, which provide the contact detection function. The function can automatically establish the most contact, just due to inappropriate part of modified and filled the missing contact, delete unnecessary contact. In the analysis tree on the left side of the Mechanical window, select "Connections", expand its contact pairs, and select "Contacts" item, then contact detection conditions appear. The "Tolerance Value" option in the diagram is the most important option to detect settings. This value is determined mainly according to the model structure, such as shell thickness, assembly conditions, etc.

Although automatic contact settings can reduce unreasonable or even superfluous constraints, some contact will not occur in the whole analysis project due to the influence of model thickness, such as the contact between the LCD screen and the shell. Because of the steel frame in the middle, the LCD screen and the shell are not contacted in practice, and the redundant contacts like this need to be deleted manually. For the missing contact automatic detection, the distance between spacing boxes and drop plates is us of the automatic range detection, so outer packaging box bottom and falling plate contact is ignored. At this time, it is needed to manually establish contact, and choose the right plane and the target plane contact.

In the automatic establishment of contact, the contact surface and the target surface are displayed in each contact area, they specify a pair of mutually contact surfaces. At this time, automatically establish contact possible contact area may not be reasonable, so it is needed to manually delete or add contact. For example, when the shell contacts, the target surface and the contact surface should be selected correctly. In this case, the target surface is only allowed to be built on the solid model. At this point, if there is a surface model in the contact, the side of the surface model must be chosen to take part in the contact with. As shown in Figure 48, the contact relationship between each body is shown.

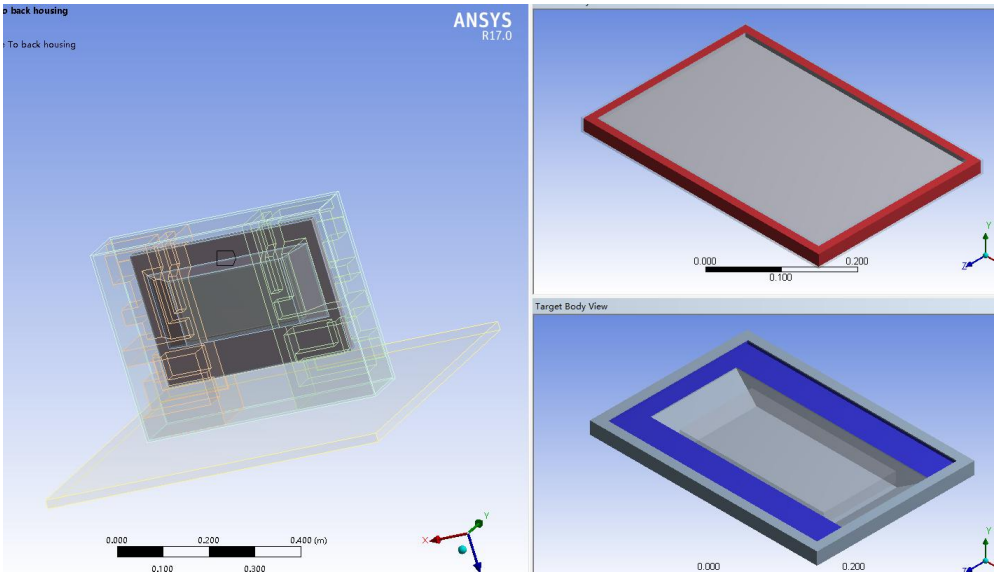

Figure 48. Contact between bodies in ANSYS simulation

Then set the contact, the display inside utilizes the binding relationship. LCD panel and steel, steel and shell, LCD and EPS, the contact type are all friction-less, as shown in Figure 49.

Details of "Body Interaction"	
Scope	
Scoping Method	Geometry Selection
Geometry	All Bodies
Definition	
Type	Frictionless
Suppressed	No

Figure 49. Friction-less contact setting in ANSYS simulation

Some problems should be paid attention to when setting the package contact:

(1) The unit of material parameters should be unified, the incorrect parameter units and parameter values will lead to the wrong contact stiffness, and eventually affect the correctness of the analysis.

(2) There is no initial contact between the surfaces that define the contact. The different parts of the model cannot overlap, and multiple contacts should not be defined between the same components.

(3) On the surface of shell quasi element, as far as possible the use of automatic single-sided contact, this contact is the easiest to define contact type, and does not cost too much time to solve.

According to the liquid crystal display package specific assembly relationship between parts, and the outer packing box, packing box and cushioning foam and foam cushion and display shell, internal packaging box and the shell of the display and display buffer foam and steel three kinds of experiments are carried out by a lot of tests the contact relation is shown in Table 5.

Table 5 Contact relationship of simulation model

Number	Contact Bodies		Target Bodies		Type
	Part	Region	Part	Region	
1	Inner steel frame	6 Faces	LCD	6 Faces	Bonded
2	Shell	7 Faces	Inner steel frame	9 Faces	Bonded
3	Shell	1 Face	Bayonet	1 Face	Bonded
4	Shell	7 Faces	Right EPS	6 Faces	Bonded
5	Shell	7 Faces	Left EPS	6 Faces	Bonded
6	Right EPS	9 Faces	5 face of package	4 Faces	Frictional
7	Right EPS	1 Face	1 face of package	1 Face	Frictional
8	Left EPS	9 Faces	5 face of package	4 Faces	Frictional
9	Left EPS	1 Face	1 face of package	1 Face	Frictional
10	Package	1 Face	Dropping plate	1 Face	Frictional

4.6. Package mesh partition

4.6.1. Mesh partition type

The mesh is the most basic element. The geometric model created is not involved in the numerical calculation and only play a supporting role for mesh computing. The nodes and units in the mesh are calculated, so meshing is needed to generate the finite element model containing nodes and elements. Therefore, the quality of mesh partition is not only related to the accuracy of calculation, but also greatly affects the computing time, and even affects the convergence of the whole calculation process. Compared with static analysis, it shows that dynamic analysis is necessary for mesh generation. The time required for dynamic analysis is much larger than that of static analysis, in addition to computing nodes. Besides, the computation time is also considered, and the computation time is directly related to the quality of mesh generation. Its relation can be expressed by means of equation (91)

$$\Delta t \le f \times \left[\frac{h}{c}\right]_{\min} \tag{91}$$

Δt is the time step, f is the time step stability factor, h is the cell size as shown in Figure 50. e is the material sound velocity. From the equation (91), it is found that the time step required for the simulation is determined by the smallest $\frac{h}{c}$ in all the units. (Geuzaine & Remacle 2009, Pp.1309-1331.) Therefore, the mesh division should avoid the time step controlled by one or more small units. In this paper, if the models were used in the model unit, due to the small thickness of shell and bayonet and other small parts, the mesh is fine, the time step is small, the computing time will need very long, up to 140 hours. Sometimes it can not be continued because of too small step size.

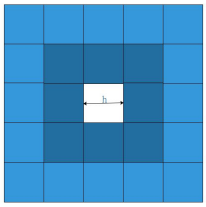

Figure 50. The effect of mesh on time step

When meshing, the physical environment of mesh target must be selected first. Workbench contains the following four physical environments: Structural Analysis (Mechanical), Electromagnetic Separation (Electromagnetic), Fluid Analysis (CFD), and Display Dynamics Analysis (Explicit), as shown in Figure 51.

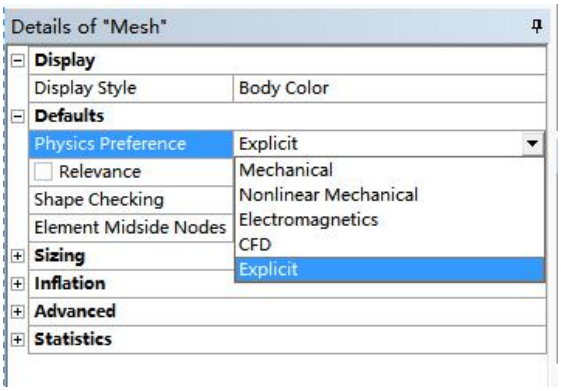

Figure 51. Physics preference of mesh

The purpose of mesh generation is to discretize the fluid and structure models, and the solution domain is decomposed into an appropriate number of units that can obtain exact solutions. In the ANSYS Workbench, mesh is used by Divide & Conquer (decomposition overcome) components geometry method which can use different methods of mesh generation. In ANSYS Workbench, 3D and 2D geometries have different meshing methods. There are some different meshing methods as shown in Figure 52. There are four meshing methods for 2D geometry of face or shell: Quadrilateral Dominant, Triangles, Uniform Quad/Tri and Uniform Quad, as shown in Figure53.

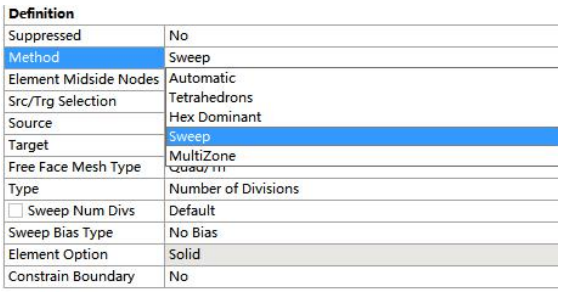

Figure 52. Mesh division method for 3D geometry

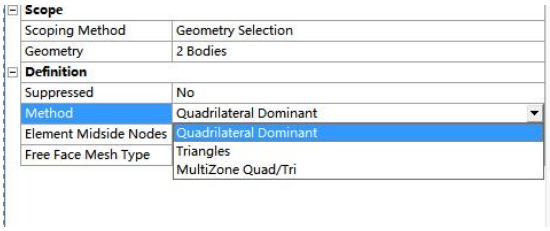

Figure 53. Mesh division method for 3D geometry

4.6.2. Mesh partition of LCD package model

We should pay attention to the following points when meshing the LCD display package:

(1) Under the condition of ensuring the time step, the mesh should be as small as possible, since it can better capture the dynamic response of the structure and capture the gradient change of stress and strain.

(2) Most of the mesh structure can be divided into tetrahedral meshes, but the preferred mesh is hexahedral element, because hexahedral element can not only reduce the computation time, but also improve the computational accuracy.

(3) For irregular shape entities, the number of hexahedral elements is increased, and the small mesh is avoided. A large number of triangular or tetrahedral elements will affect the computational accuracy and convergence of the display analysis.

(4) We need to pay attention to efficiency, a lot of trial elements need more computing resources (memory, run time), and the mesh partition needs to balance the analysis accuracy and resource usage.

(5) Define or accept a few global mesh sizes as default values.

When meshing each part of LCD display package, the method of mesh division of each component is shown in Table 6. Control the size of the model of buffer foam and surface (shell and internal steel). Since each element size is same when meshing the component, it is conducive to the calculation and analysis, and can get a reasonable mesh, so the mesh size is controlled into 20 *mm*. In the meshing of the buckle, it is refined because it plays a major role in the transmission of the shell and the internal steel frame. Figure 54 showed the final mesh division. (Moaveni 2011 Pp.224-228.)

Table 6 Meshing method for each component

Number	Model	Meshing method
1	Outer box	Multizone
2	Cushioning foam	Hex Dominant
		Body Sizing:20*mm*
3	Shell &Internal Steel Frame	Uniform Quad:20*mm*
4	Bayonet	Body Sizing;1*mm*

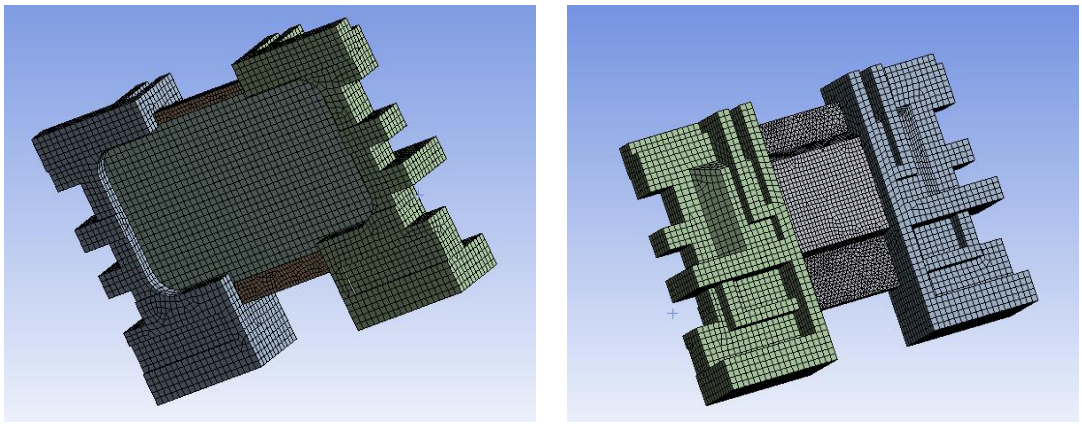

Figure 54. Mesh division for LCD

4.7. Boundary condition settings and solving

ANSYS Workbench provides gravity acceleration, acceleration, angular acceleration, torque, pressure, fixed support and other settings for the simulation of the environment. According to the drop principle, this subject simulates the drop environment, the settings are mainly in the following four aspects shown as Figure 55:

(1) Fixed drop plate. According to the actual situation, we simulate the drop plate as ground. During the whole drop process, the drop plate is fixed.

(2) Adding gravity field. Gravity is the driving force of drop simulation. So there is a need to set the direction and size of gravity acceleration according to the direction of fall, which can be implemented by adding "Standard Earth Gravity". The system defaults all the geometric models are in the gravity field. Adjusting the direction of gravity acceleration is consistent with the direction of the package falling.

(3) Adding speed. According to the calculation above, it is necessary to add the speed of 3904*mm/s* to all the models in the model to remove the drop plate. Define speed by "Velocity" and adjust the direction of the package falling direction to make it consistent.

(4) Analysis item setting. Mainly set analysis time, which is from the beginning of the fall to the end of the selected time. To make sure accurate analysis to the whole drop process, in this project, the change of package in 4ms time is analyzed time after the start of the fall.

When the setup is complete, the model state is shown in Figure 55. At this point, the pre-processing settings of the liquid crystal display package drop simulation set up. Select the shortcut key "Solve" in the window to solve, the message "LS-DYNA keyword file has been created" will appear soon in the message window, which indicates that the K file has been generated and stored in a folder named "MECH".

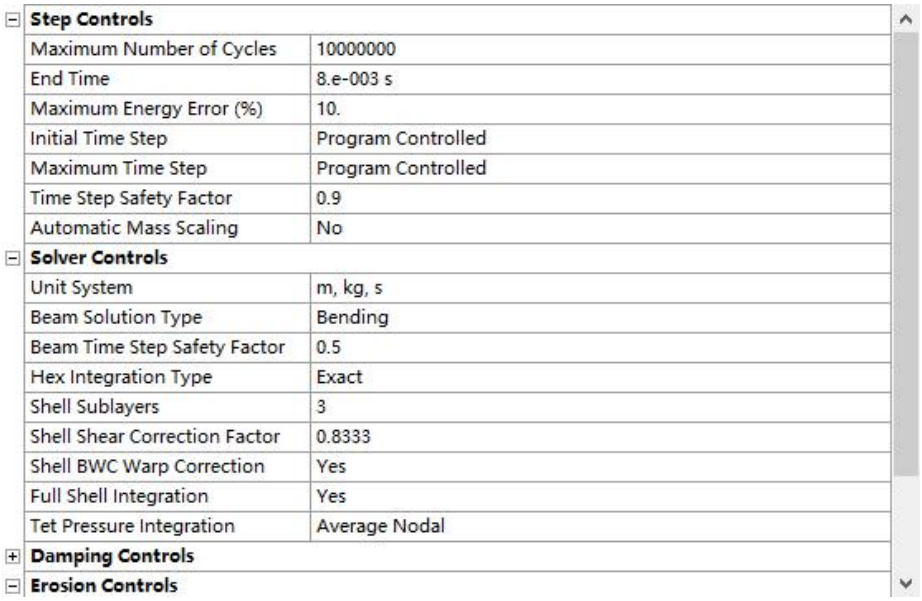

Step Controls	
Maximum Number of Cycles	10000000
End Time	8.e-003 s
Maximum Energy Error (%)	10.
Initial Time Step	Program Controlled
Maximum Time Step	Program Controlled
Time Step Safety Factor	0.9
Automatic Mass Scaling	No
Solver Controls	
Unit System	m, kg, s
Beam Solution Type	Bending
Beam Time Step Safety Factor	0.5
Hex Integration Type	Exact
Shell Sublayers	3
Shell Shear Correction Factor	0.8333
Shell BWC Warp Correction	Yes
Full Shell Integration	Yes
Tet Pressure Integration	Average Nodal
Damping Controls	
Erosion Controls	

Figure 55. Boundary condition setting

This project selects LS-DYNA Solver for environment, and the license file selects the first ANSYS Multiphysics/LS-DYNA. In the Keyword Input File, select the folder where the IC file is located. When the setting is finished, the "Run" is selected to solve the problem until the prompt of the arrival termination time appears in the interface, which indicates that the solution is completed.

4.7.1. Drop simulation result and analysis of LCD package

Although ANSYS LS-DYNA has powerful computing function, the subsequent processing function is relatively poor, so joint modeling is commonly used, as shown in Figure 56. LS-PREPOST is used to analyze with ANSYS. LS-PREPOST is a pre-processing and post-processing software dedicated to LS-DYNA3D developed by LSTC company, and the

post-processing function of this software is very powerful. (Pan & Chen 2007, Pp. 2249-2259.)

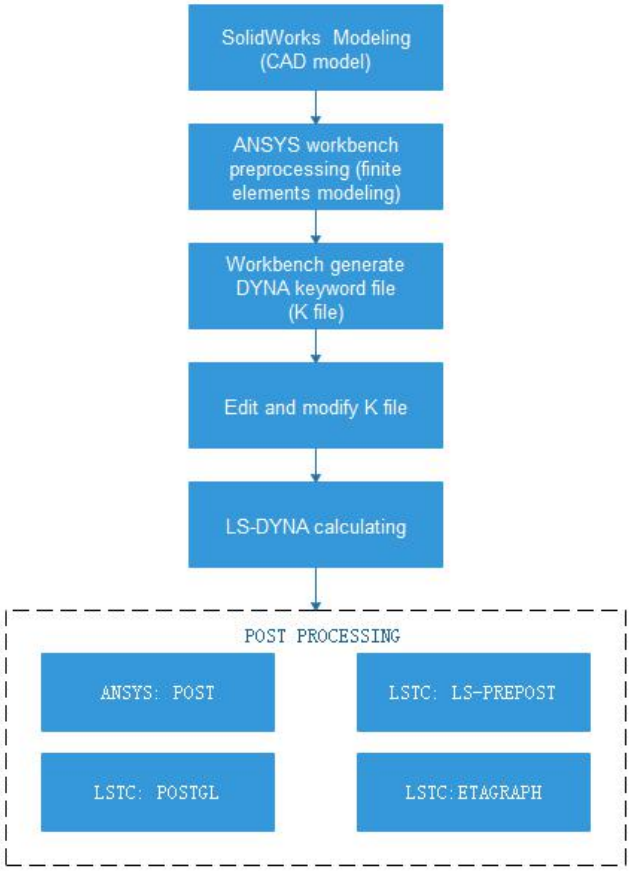

Figure 56. Solidworks modeling-Workbench-DYNA joint modeling solution flow

When the LS-DYNA3D solver is used, the units with different physical quantities must be coordinated, that is the units of basic physical quantities and other units derived from them must be unified. For structural analysis, the basic physical quantities are length, mass and time. In the process of calculation, LS-DYNA3D does not limit what kind of unit system must be used, and even users can create a unit system themselves. If the rank is coordinated, the unit of calculation is definite. For example, in structural analysis using the basic units of *M, kg, s,* then the calculated pressure unit must be *Pa*. The length, quality and time units selected are mm, kg and s respectively. In this paper, the calculated speed is

mm/s, the acceleration unit is mm/s^2 and the deformation unit is *mm*. Understanding the unit problem in LS-DYNA3D can be used to analyze the simulation results. (Pan & Chen 2007, Pp. 2249-2259.)

4.7.2. Bottom drop simulation results

In addition to the packaging components, the deformation of the internal display can also be studied, for example: the deformation of the LCD rear shell in Figure 57. It can be seen that the deformation of the middle part of the rear shell is the largest, and the deformation of the foam is smaller because of the protection of the buffer foam, and the deformation of the lower part of the rear shell is generally smaller than the deformation of the upper part. This is mainly due to the structure of buffer foam. The material of lower part is more than the upper part of cushioning foam, which can be better to absorb shock and protect the built-in products.

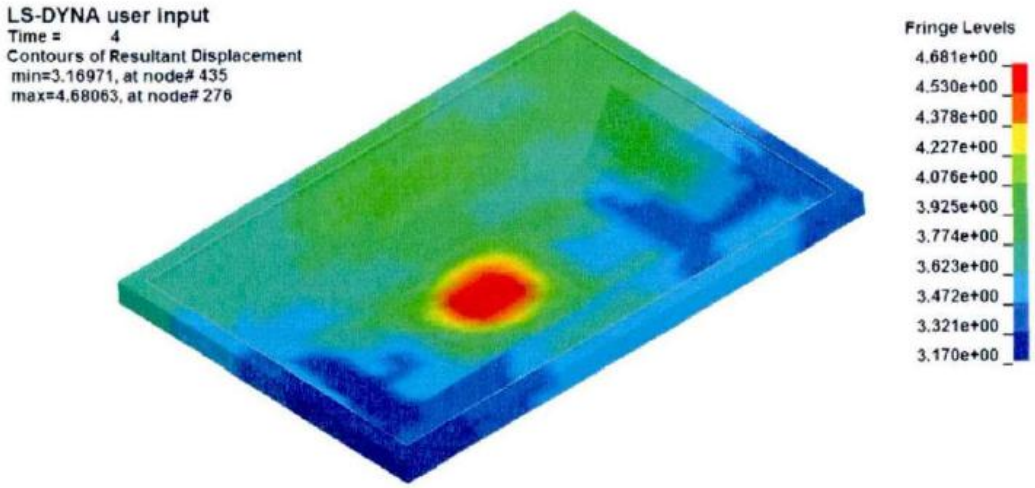

Figure 57. Deformation nephogram of LCD rear shell

As shown in Figure 58, the maximum acceleration of the LCD package appears in the buckle of the product shell, the maximum value is 11051.4 mm/s^2, that is 1.10514*g*<24*g,* which also means it is less than the international specification of product fragility G; left figure is the maximum acceleration of the housing buckle amplification diagram. The

maximum acceleration occurs on the buckle. The main reason is that the slot is the main part of the connecting shell and inner steel frame. The energy transfer of the two parts is mainly accomplished by the card groove, and the buckle size is small, for larger energy transfer, the speed changes faster, so the acceleration value will be larger.

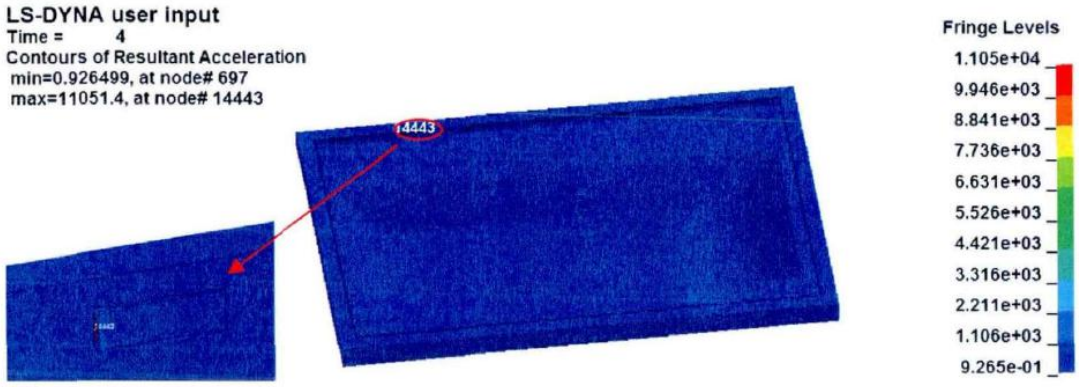

Figure 58. The most acceleration of LCD package

4.7.3. Simulation results of short side drop

When the short side falls, the maximum acceleration of the package is 191083 mm/s^2, which is 19.1083g<24g. Its product fragility is less than international regulations. Figure 59 shows the maximum acceleration profile. From the graph, the maximum acceleration is distributed on the snap side of the shell. Compared with the bottom drop, the maximum acceleration values are distributed on the buckle of the shell, but the drop acceleration on the short side is larger than that on the bottom. Because in the rebounding process, the package will tilt, bottom buckle will connect shell and internal steel frame to transfer larger energy.

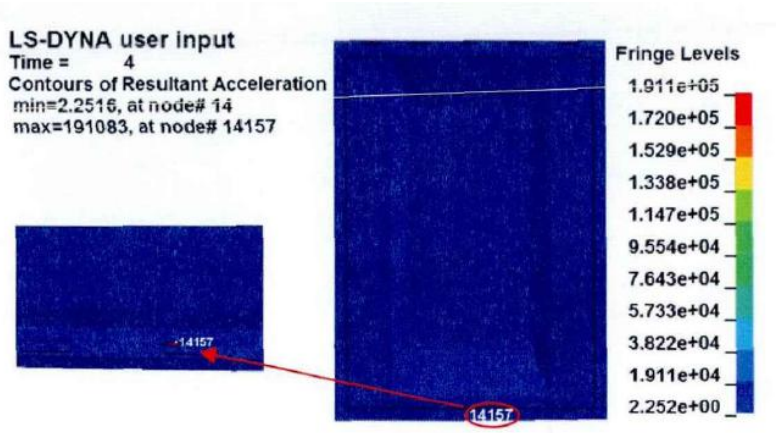

Figure 59. Maximum acceleration distribution

Figure 60 shows the acceleration profile of the LCD screen. The maximum acceleration is distributed on the edge of the impact side of the LCD screen, which also proves that the vulnerable parts such as LCD glass are prone to breakage near the four corners in the impact process.

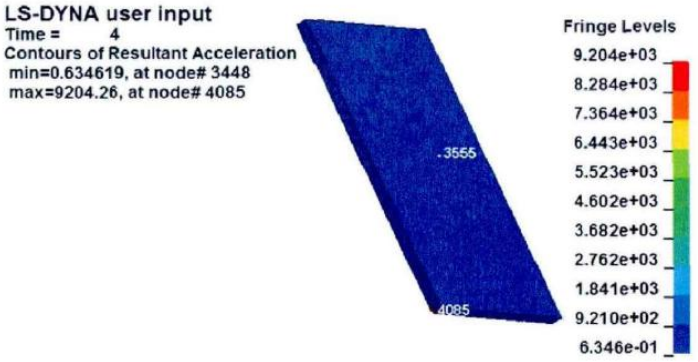

Figure 60. Acceleration map of LCD screen

4.7.4. Simulation results of long side drop

Figure 61 shows the deformation figure of the 5001 nodes at the bottom of the buffer foam. From the graph, the deformation of the node increases from zero to 1.58mm in the 0-0.4ms time interval. At this time, the package falls to the falling plate at a given speed, and the slope of the line is the speed of the package. In the 0.4ms-0.75ms period, the carton impacted by the downward compression carton, the carton began to deform, and the

deformation of the node continued to increase with a small slope. When 0.75ms reaches 1.75mm, the carton is compressed to the minimum, and the deformation reaches the maximum. In the 0.75ms~1.6ms time, the deformation of the node decreases, indicating that the buffer foam begins to compress. At 1.6ms, the buffer foam reaches the maximum deformation and is compressed to the minimum. After 1.6ms, the deformation of the node increases, and then the cushioning foam begins to rebound.

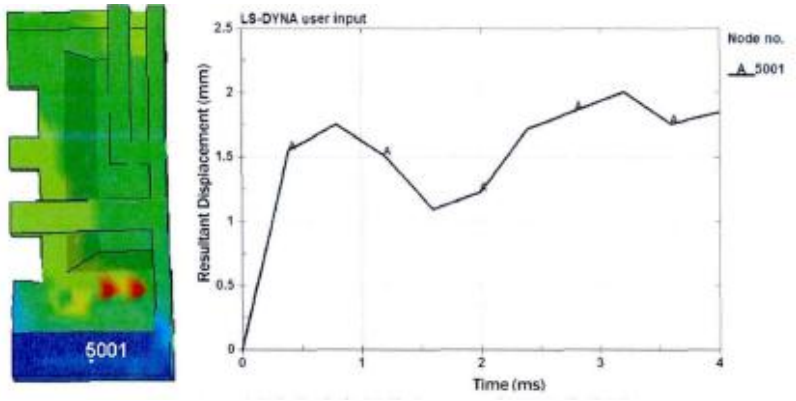

Figure 61. Cushioning foam bottom node 5001 deformation curve

Like the bottom drop, the maximum acceleration of the LCD package also appears on the buckle of the product shell. As shown in Figure 62, the maximum acceleration value is 45942.4 mm/s^2, which is 4.59424g<24g. which means that it is less than the international standard product brittleness G. Compared with the bottom drop, the maximum acceleration of the package increases, which is due to the limitation of the reinforcing ribs at the bottom of the buffer foam when the side falls, and the reinforcing ribs play a good buffering role when the bottom surface falls. In addition, it may be related to the center of gravity of the package. When the long side falls, because the center of gravity of the package is biased, during the process of the rebound, the package inclines, and the buckle connects the shell and the inner steel frame, so it is more likely to produce greater acceleration.

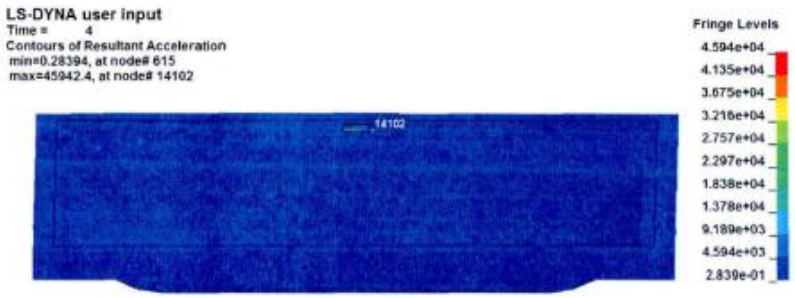

Figure 62. The biggest acceleration distribution Pavilion

Package main components of strain nephogram is shown in Figure 63. The strain nephogram of the display case is shown in Figure 63(a). The maximum strain is 27272 $\mu\varepsilon$, which appears on the buckle of the shell. Figure 63(b) shows the strain nephogram hidden buckle after the shell of the display, the maximum strain value is 389.38 $\mu\varepsilon$, the inclined part strain display shell rearward protrusion value. Figure 63(c) is shown in the display frame strain-nephogram from the figure, in the groove of the upper part the strain is the largest, reached 1047.06 $\mu\varepsilon$, the maximum strain on the shell also appeared in the card slot corresponding to the fastener. Figure 63(d) shows the LCD screen display the strain-nephogram from the figure, the LCD screen strain nephogram is symmetrical, the maximum strain value is 39.2091 $\mu\varepsilon$, appeared in the fall at the side of the corner. It is further shown that the vulnerable parts such as LCD glass are prone to be damaged near the corner of the impact parts during the impact process. The maximum strain of each part of package is compared: The maximum strain of the inner product is obviously smaller than that of the outer buffer foam, which indicates that the external cushioning package has a good protective effect on the built-in product.

(a) Strain nephogram of display shell

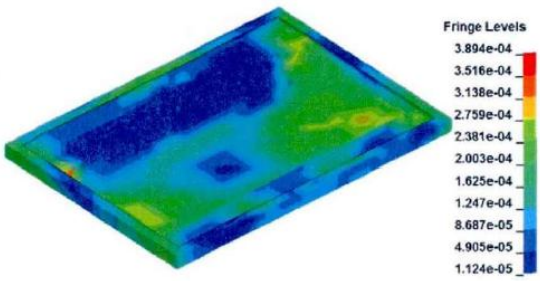

(b) Strain nephogram of display shell(hidden clasp)

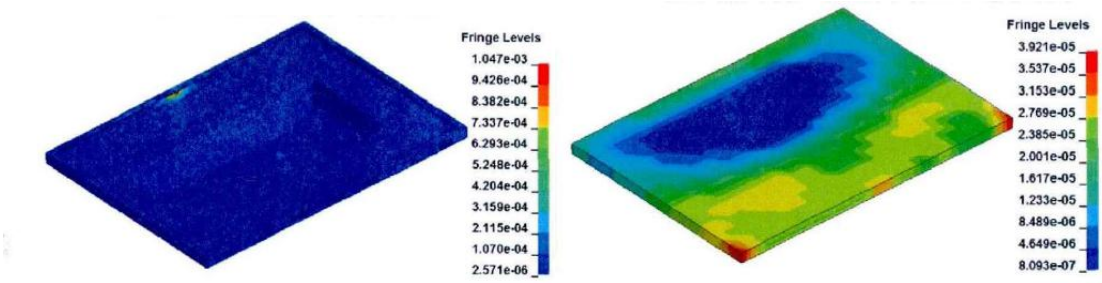

(c) The display frame strain nephogram (d) The liquid crystal display screen strain nephogram

Figure 63. Strain nephogram of main components of package

4.7.5. Simulation results of edge drop

When the edge falls, the maximum acceleration of the package is 1665.73 mm/s^2, which is 0.166573g<24g. Product fragility is less than international regulations. Figure 64 shows the maximum acceleration profile. As you can see from the figure, the maximum acceleration is distributed on the corner of the back stiffener. From the figure, the back acceleration is larger than the front, which is caused by more shock on the back. Select two nodes at the bottom of the two buffer foam, as shown in Figure 65. The acceleration curve is shown in figure 66. From the figure, the curve of two curves is basically the same, and reaches the maximum at 0.75ms, which occurs in the early stage of the drop process.

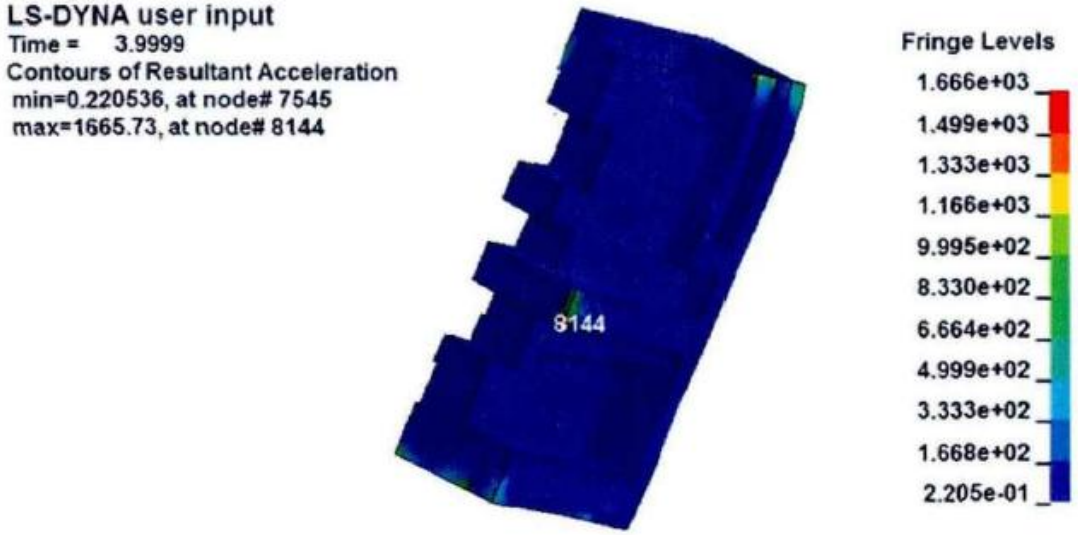

Figure 64. Maximum acceleration distribution map

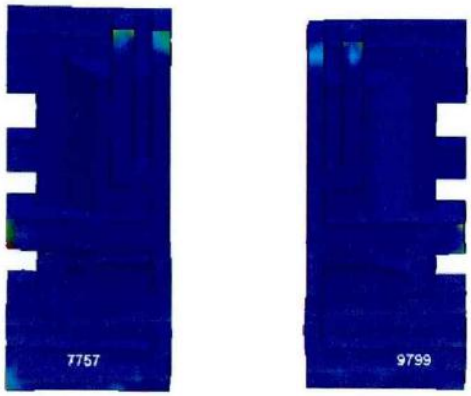

Figure 65. Acceleration curve of the cushioning foam

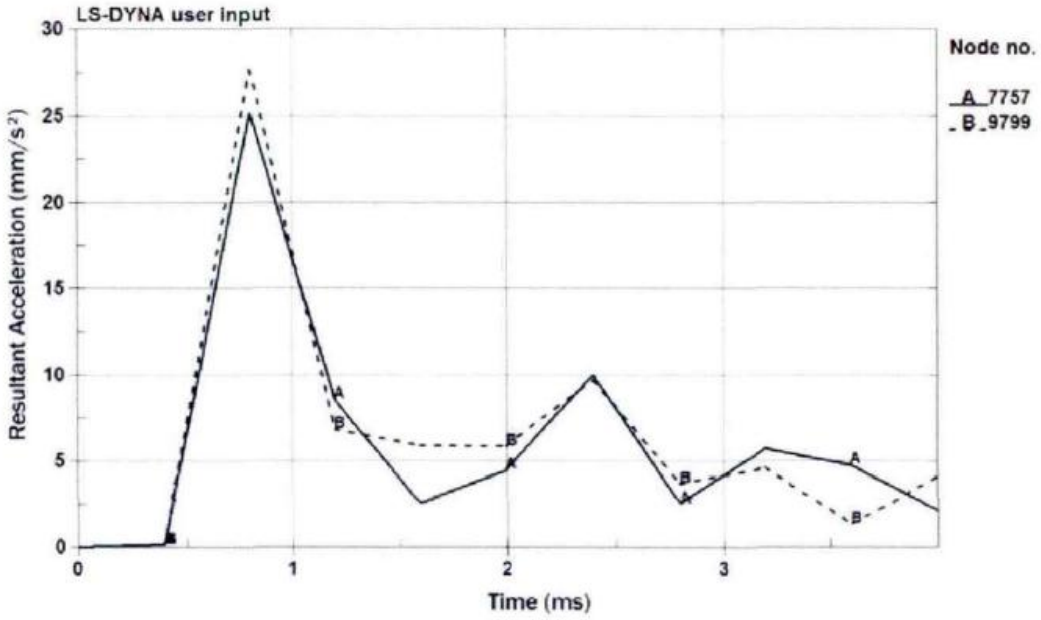

Figure 66. Acceleration curves of back nodes of cushioning foam of 7757 and 9799

Figure 67 shows the acceleration profile of the shell. From the figure, the maximum acceleration of the shell is 1341.07 mm/s^2, which is distributed in the buckle of the shell. Figure 68 shows the acceleration image of the LCD screen. From the figure, the maximum acceleration is distributed on the corner of the upper part of the LCD screen, which also proves that the vulnerable parts such as LCD glass are prone to breakage near the four corners in the impact process. In the middle part of the LCD screen, select a node 6337, the acceleration curve of the node in Figure 69. The acceleration value of the LCD screen in

the early drop is small, the maximum acceleration value is about 3.6, and it appears in the rebound stage, which shows that when the edge falls, the internal product of the package is easy to damage in the rebound stage.

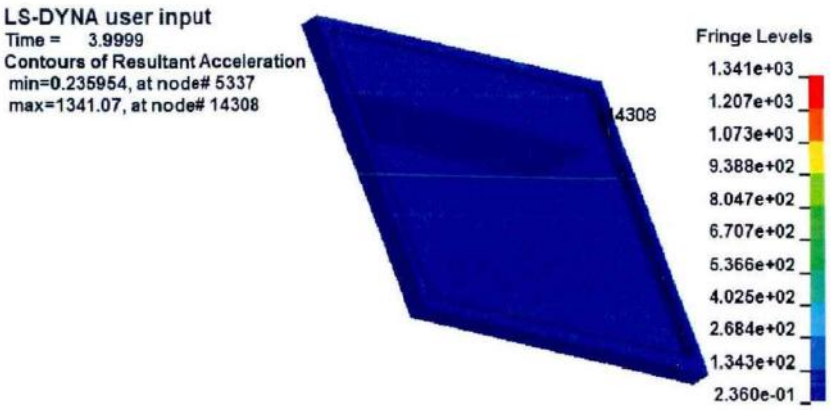

Figure 67. Acceleration nephogram of shell

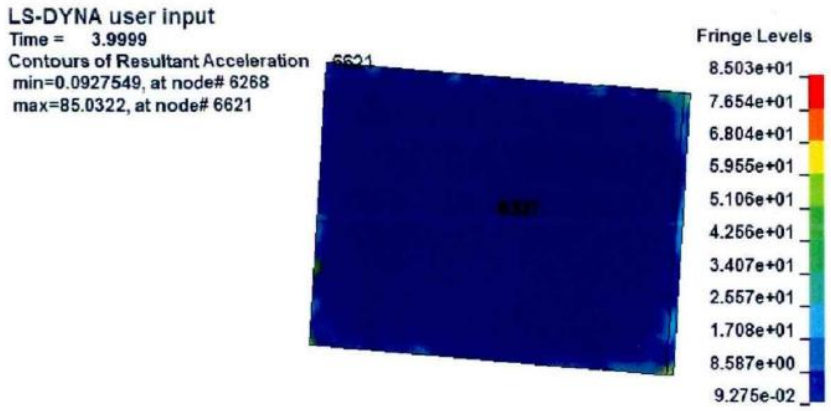

Figure 68. Acceleration nephogram of LCD screen

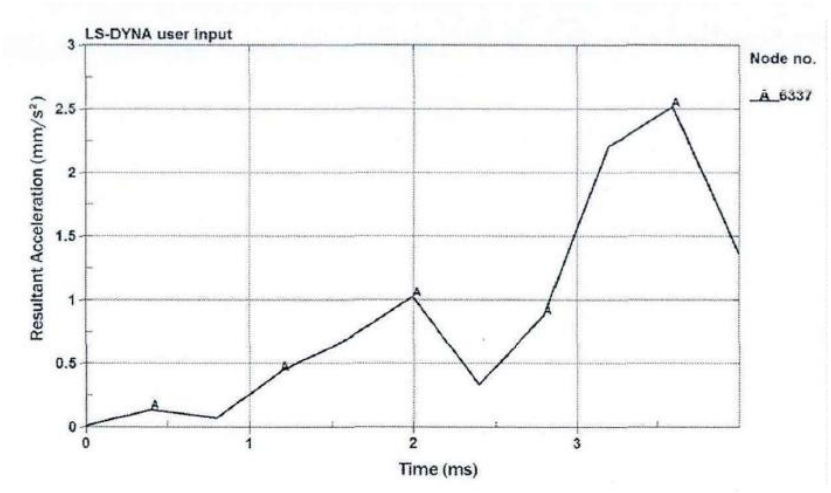

Figure 69. Acceleration curve of display center node of 6337

5. EXPERIMENTAL STUDY

Experimental study is always needed when verifying the correctness of the hypothesis, so in this paper, some dynamic and static experiments are carried out and analyzed.

5.1. Test on dynamic cushioning performance of materials

The dynamic compression test of cushioning packaging materials is used to evaluate cushioning performance of cushioning materials under impact and its protection ability for inner packaging products in circulation process. The impact loaded on the cushioning packaging material is applied in the test with a free drop weight hammer. The impact of the cushioning packaging material in the loading and unloading process is simulated. The test results are shown as the dynamic buffering performance and the curve of the cushioning packaging material. This section studies the cushioning performance of the new mono-layer polyethylene cushioning material, compares the cushioning properties of the commonly used environmentally friendly cushioning packaging materials under the same conditions. (Sims & Bennett 1998, Pp.134-142.)

5.1.1. Dynamic buffer performance testing system

The testing system of dynamic buffer performance tester is composed of buffer material testing machine, accelerometer, charge amplifier, data acquisition and data processing system, as shown in Figure 70. The real material testing machine is shown in Figure 71. The test machine should have a free drop weight (the weight hammer should be attached to the acceleration sensor) and a large base of the base. The weight of the heavy hammer is flat and can fully cover the impact surface of the test sample, and its quality can be adjusted. The heavy hammer should be hard and have enough stiffness to ensure that the test waveform is distorted in the impact process without the vibration of the weight of the

weight. The base of the test machine should have sufficient stiffness, and its quality is at least 50 times the mass of the maximum weight.

The sample is placed in the center of the base, and a fixed weight and acceleration sensor are fixed on the impact platform. When lifting device is used to lift the impact platform to a predetermined height, the lifting device releases the hook from the impact table, and the impact table drops freely along the guide post. The impact acceleration signals to the weight of the first acceleration sensor to collect the sample dropped, after converting accelerometer charge to the charge amplifier, the output voltage of the charge amplifier (Analog) by A/D converter into a digital signal, stored in the computer memory, computer software, display acceleration time. Curve, shock wave and shock duration and maximum acceleration. (Goyal & Buratynski 2000, Pp.45-52.)

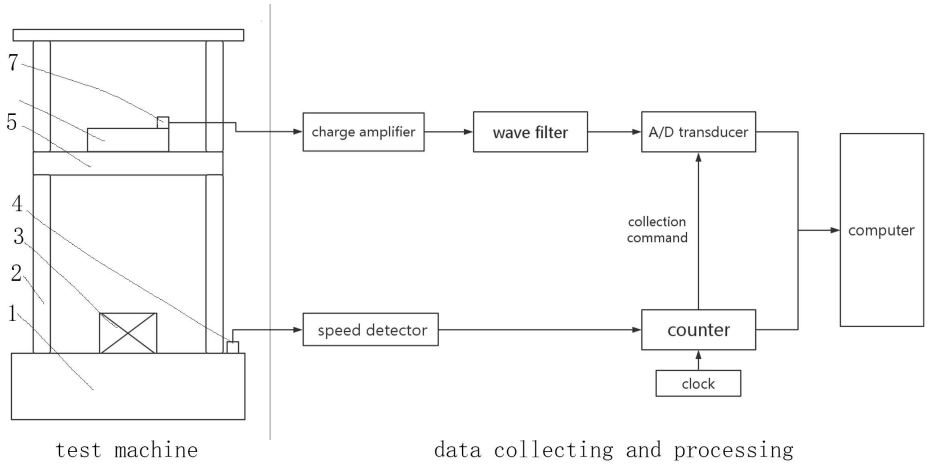

Figure 70. Dynamic Characteristics Testing Machine for Cushioning Materials

(1 Base 2 Guide Column 3 Sample 4 Light-emitting Diode 5 Impact Table 6 Weight 7 Acceleration Sensor)

Figure 71. Testing Machine for Cushioning Materials

5.1.2. Test objects and steps

1) Dynamic buffer compression test object

The dynamic cushioning compression test objects are new single layer polyethylene cushioning materials, and commonly used environmental protection cushioning packaging materials, such as corrugated cardboard, honeycomb paperboard, air cushion packaging, etc.

2) The manufacture and treatment of the sample

The sample is extracted from the sample for more than 24 hours, and the number of each sample is not less than 5. The sample is a regular rectangular shape, the upper and lower dimensions of 10cm×10cm. Two kinds of EPE materials with different densities are 2.5cm, 5cm, 7.5cm and 10cm, respectively. Two kinds of drop heights are obtained from 60cm and 90cm. Table 7 provides detailed parameters of the EPE samples as shown in Figure 72. The test parameters of corrugated cardboard, EPE and honeycomb cardboard as shown in Figure 73 are set as Table 8, and the thickness of the liner is 2cm, and the drop height is 40cm.

Table 7 Parameters of Dynamic Characteristic Test for EPE

Sample	Density $\left(kg / m^3\right)$	Length × Width (mm)	Thick (mm)	Drop Height (cm)
EPE220	31	100 × 100	25 50 75 100	60
			50 75 100	90
EPE400	70	100 × 100	25 50 75 100	60
			50 75 100	90

Figure 72. EPE samples for *Dynamic Characteristic Test*

Table 8 Parameters of Corrugated Board, EPE Mats and Honeycomb

Sample	Length × Width (mm)	Thick (mm)	Drop Height (cm)
AB Corrugated Board 200/180A/150B/200 g / m^3	100 × 100	20	40
A Corrugated Board 180A/250/180 g / m^3	100 × 100	20	40
Honeycomb	100 × 100	20	40
EPE220	100 × 100	20	40

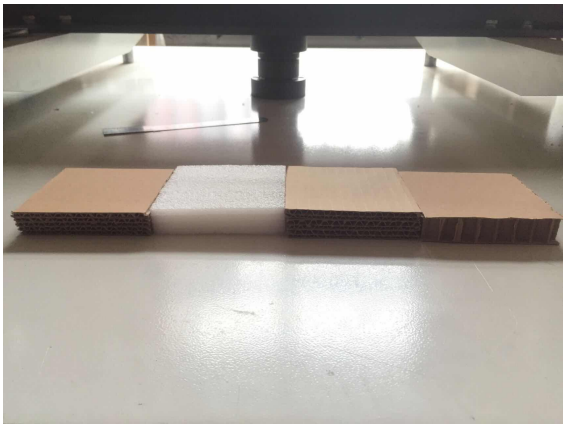

Figure 73. Four different test samples

3) Test Procedure

a) The sample is placed on the base of the buffer tester, and the center of the sample is placed on the same vertical line with the center of gravity of the impact platform. The sample is properly fixed, but the specimen cannot be deformed.

b) The impact table of the predetermined load falls from the predetermined equivalent drop height, and the impact specimen is impacted 5 times continuously, and the time interval of each impulse is 2min. The acceleration of each impact, the time curve, and the maximum average acceleration of the 4 shocks are calculated.

c) All samples were tested in accordance with the above methods. According to the needs, the weight quality, the sample thickness and the equivalent drop height on the impact table are changed.

5.1.3. Test results and analysis

The maximum acceleration and static stress data of the foamed polyethylene are measured by the test, as shown in Table 9.

Table 9. Testing Date of EPE

Number	Drop Height mm	Gasket Thickness mm	Static Stress (kPa)	1.7	2.2	3.9	6.9	9.8	11.8	13.8	17.2
EPE 22060	600	25	Max Accelarations (g)	75	70	62	67	79	100	120	
		50		42	40	36	32	31	32	33	37
		75		36	33	27	24	22	21	20	21
		100		30	28	21	19	17	16	16	15
EPE 22090	900	50		60	57	49	47	51	57		
		75		42	41	36	32	31	32	34	37
		100		33	32	29	25	24	23	24	25
EPE 40060	600	25		120	90	62	65	60	79	88	109
		50		85	67	52	35	28	27	28	32
		75		80	63	42	31	24	22	19	18
		100		78	56	35	27	22	20	17	15
EPE 40090	900	50		120	90	60	42	44	448		
		75		85	67	52	35	29	27	28	31
		100		75	55	46	33	25	22	21	21

The dynamic compression test data for several common environmental cushioning materials under the same condition are shown in Table 10, Table 11 and Table 12.

Table 10 Testing Data of Corrugated Board

Sample	Static Stress (kPa)	Maximum Acceleration (g)
AB Corrugated Board	0.69	200
	0.98	145
	1.18	171
	1.47	250
	1.57	278
A Corrugated Board	0.98	153
	1.47	150
	1.96	190
	2.45	267

Table 11 Testing Data of EPE220

Sample	Static Stress (kPa)	Maximum Acceleration (g)
EPE220	1.7	70
	3.4	48
	6.9	42
	10.3	50
	12	56
	13.7	64

Table 12 Testing Data of Honeycomb

Sample	Static Stress (kPa)	Maximum Acceleration (g)
Honeycomb	0.4	200
	0.98	150
	1.96	60
	2.94	50
	3.92	40
	4.9	50
	5.88	65

5.2. Drop test of transport package

This section verifies the finite element simulation model by simulating the loading and unloading environment of the package.

5.2.1. Summary of drop impact test

Drop impact test include cushion, hook type, double plate and rotary wrist etc. This section adopts the rotary wrist drop test machine. When the test is carried out, when the sample is raised to the specified height, the revolving wrist drops suddenly and turns and contracts. Get out of the sample, according to the predetermined state of free fall, collision and impact surface impact.

The drop impact test system consists mainly of accelerometer, charge amplifiers, data acquisition cards and computers, such as Figure 74. When the sensor falls with the test

piece, in the process of impact, the sensitive mass in the sensor feels the acceleration to produce a positive ratio of inertia force. The acceleration is indirectly measured by changing the inertia force into strain, stress, or by the conversion of the piezoelectric element into the charge amount by the elastic element. The charge amplifier produces a voltage proportional to the amount of charge, and matches the A / D conversion, and then sends it into the data acquisition card. The data is read out by the software system for data processing. (Guo, Xu, Fu & Zhang 2010, p.378)

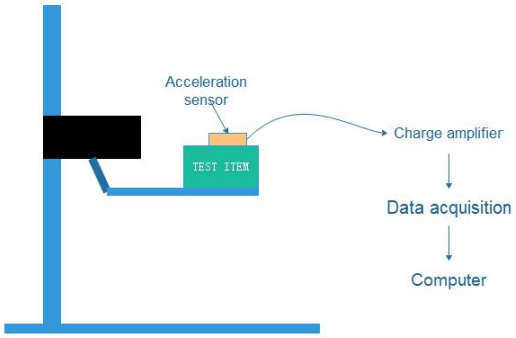

Figure 74. Drop Test System

5.2.2. Test equipment

This test adopts the drop impact test machine produced by Lansmont company, as shown in Figure 75. The software is designed and developed by Lansmont company. Figure 76 is a test system photo.

Figure 75. Drop Test system

Figure76. Photo of Drop Test System

5.2.3. Steps of the test

The purpose of the test

The drop impact test of the package is carried out by simulating the real falling impact environment of the cushioning package of the LCD display as shown in Figure 77. The reliability of simulation analysis of package drop impact is verified through experiments and lays the foundation for future better and more accurate simulation of cushioning package.

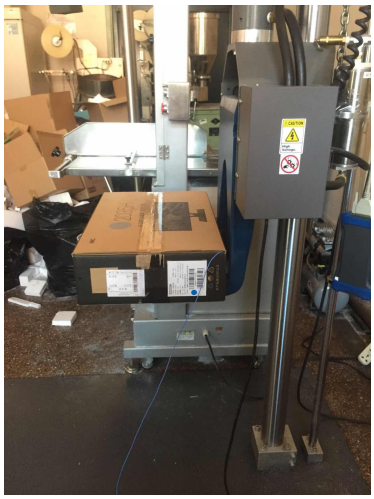

Figure 77. Dropping test for LCD display

Test steps

1) According to the ISTA 3A standard, the drop height of the package was determined to be 770mm, and the height of the revolving wrist of the buffer drop impact test machine was adjusted to 770mm.
2) The package is placed on the wrist of the drop impact tester according to the expected fall mode (surface drop and angle drop), and accelerometer is placed on the upper surface of the product.
3) The acceleration sensor is connected to the charge amplifier, the charge amplifier and the signal acquisition card connected to realize the data recorded by the computer through the data of chestnut truck.
4) The swing wrist of the impact tester is released suddenly, so that the package will fall freely according to the predetermined condition, and it will collide with the impact platform to form impact and record the drop impact data.

5.2.4. Analysis of test results

The response curve of the face drop and corner drop of the package is shown in Figure 78 and Figure 79.

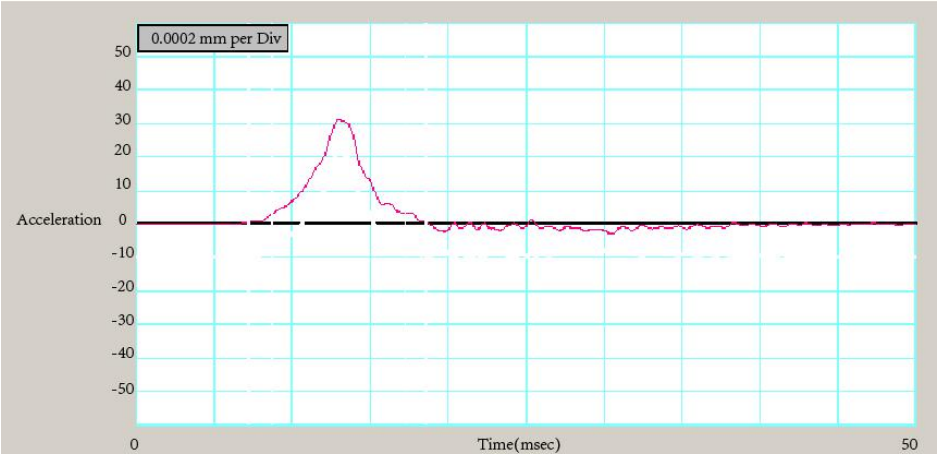

Figure 78. Drop Test Sequence-Face

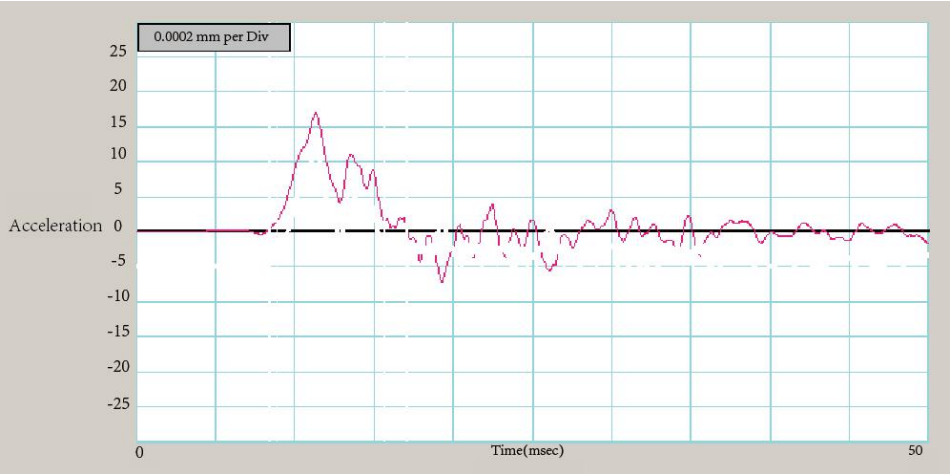

Figure 79. Drop Test Sequence-Corner

The data of the test results are shown in Table 13.

Table 13 Testing Data of Drop Test

Maximum Acceleration	X (G)	Y (G)	Z (G)
Drop Test Sequence-Face	2.6	32.8	3
Drop Test Sequence-Corner	14.1	17.4	6.5

Because of the drop impact, the acceleration response in the vertical direction of the product is mainly considered. Therefore, the test data in the vertical direction of the product are compared with the simulation results, as shown in Table 14.

Table 14 Testing Data of Drop Test

Maximum Acceleration	Test Value	Simulation Value	Relative Error
Drop Test Sequence-Face	32.8	35	6.7%
Drop Test Sequence-Corner	17.4	19	9%

From the analysis of the test results, the relative error between the results of numerical simulation analysis and the test value is about 8%. Because of buffer simulation model does not take into account the outer corrugated packaging for products, there are some differences between the parameters of ground material parameters and finite element

model, and the drop test itself has the test error and other factors, so the drop simulation cushion package analysis model is basically correct.

5.3. Conclusion

In this chapter, the buffer performance of a new type of single layer polyethylene buffer material is tested by the dynamic buffering test of material. Under the same condition, the cushioning properties of the commonly used environmental cushioning packaging materials are compared. By simulating the real drop impact environment of the specific products, the drop impact test of the package is carried out, and the drop test value is compared with the simulation results, which verifies the reliability of the finite element analysis.

6. RESEARCH ON THE DESIGN METHOD OF CUSHIONING PACKAGING

Buffering performance of modern cushioning packaging material, theoretical analysis method of nonlinear packaging and numerical simulation analysis method of cushioning packaging are analyzed in previous chapters. Based on the results of this study, how to apply these theories and analytical methods to the actual cushioning packaging design is discussed in this chapter. To enrich and improve the existing cushioning packaging design system, the relevant enterprises and individuals provide methods and basis for the selection of cushioning packaging materials and the design of cushioning packaging and the performance evaluation of the transport package.

6.1. Design method of traditional cushioning packaging

During circulation and transportation, the product will be affected by various external harmful factors. Although the product itself has a certain ability to resist these harmful factors, in general, the damaged strength of the product is less than the strength of the harmful factors of the outside world, and the product will be damaged in the process of circulation. Therefore, the purpose of the cushioning packaging design is to select the appropriate buffer material. A reasonable buffer structure is designed to absorb and obstruct the shock and vibration of the outside world, to ensure the safety of the inside product.

Generally, the environmental hazards encountered in the process of circulation are falling, vibration, shock, temperature, humidity, static pressure, static electricity and so on. Among them, the phenomenon of product damage caused by vibration and shock is the most common. Therefore, when designing cushioning packaging, we must first determine the product's circulation and transportation environment, mainly to determine the equivalent drop height and the vibration condition during the product circulation.

The product itself has a certain ability to resist the dangers of the outside world, which can be described by the product's crisp value. Brittle value, also known as vulnerability, reflects the ability of products to withstand external forces. Generally, the maximum acceleration value that can be sustained by the product itself or its components is expressed by G_m .The greater the G_m value, the stronger the ability of the product to bear external force. But the factor that can bear the maximum acceleration cannot fully express the impact strength of the product. But the factor that can bear the maximum acceleration cannot fully express the impact strength of the product. Therefore, the concept of impact damage boundary curve is put forward, which fully reflects the relationship between acceleration peak value, velocity variation, pulse waveform and product breakage, and further illustrates the impact resistance capability of products.

The good cushioning performance of the cushioning package is mainly achieved by absorbing external shocks by the cushioning pad. However, due to the non-linearity, large deformation and damping of the cushioning material, it is difficult to get the theoretical solution of the packing dynamic differential equation to guide the cushioning packaging design. Therefore, the experiments are carried out to solve the design problem of cushioning package, that is, the drop impact test of the combination system of the product and the cushioning material is carried out and a buffer characteristic curve is used to characterize the buffer characteristics of a combined system. So many experiments are needed to obtain the buffering characteristics of each material under the different height of falling. Then, the designer can carry out a comprehensive or partial cushioning package design for the product according to the circulation environment and product characteristics. Through the experiment, the packaging is checked, and the cushioning packaging design is completed.

There are five steps to design the cushioning package:

(1) Determine the environmental conditions;

(2) Determine the product crisp value;

(3) Selection of buffer materials

(4) Design prototype packaging structure;

(5) Test evaluation prototype packaging

Then, based on the "five steps", people put forward the "six steps", The only difference between the two is that the latter has added a new step "product redesign" between the second and the third steps of the former. If the fragility value of products that have been designed and manufactured is inappropriate or unreasonable, it will urge people to consider redesigning products and improving product fragility.

Traditional cushioning packaging design requires cushioning packaging design with sufficient cushioning material characteristic curve and establishing a complete buffer material characteristic curve library, to effectively carry out cushioning packaging design. But the cushion curves are drawn materials requires a lot of manpower, material and financial resources, due to the limitation of experimental conditions, the cushion curves for many materials are not complete, especially in Chinese production of packaging materials many also do not have the ability to provide material cushion curves. Therefore, it is very important to establish a perfect curve Library of the characteristics of the cushioning material. (Azzi, Battini, Persona & Sgarbossa 2012, Pp.435-456.)

6.2. Nonlinear theory analysis of cushioning packaging

With the further research of packaging dynamics, the theoretical solution of nonlinear cushioning packaging dynamic equation to the cushioning packaging design is applied, and the impact waveform and impact duration of cushioning packaging is analyzed. According to the theory of product brittleness, the impact acceleration, shock wave and impact time are the main causes of product damage. Therefore, the cushioning performance of the

package can be evaluated conveniently and quickly according to the result of the analysis of the cushioning package theory.

In the fourth chapter, the theoretical analysis method for solving the drop impact response of nonlinear packaging is given, and the solution equation is derived. With the help of computer technology, the impact waveform and impact duration of cushioning packaging can be easily solved. The theoretical analysis and evaluation of the cushioning performance of nonlinear packaging is carried out, which is shown in Figure 79.

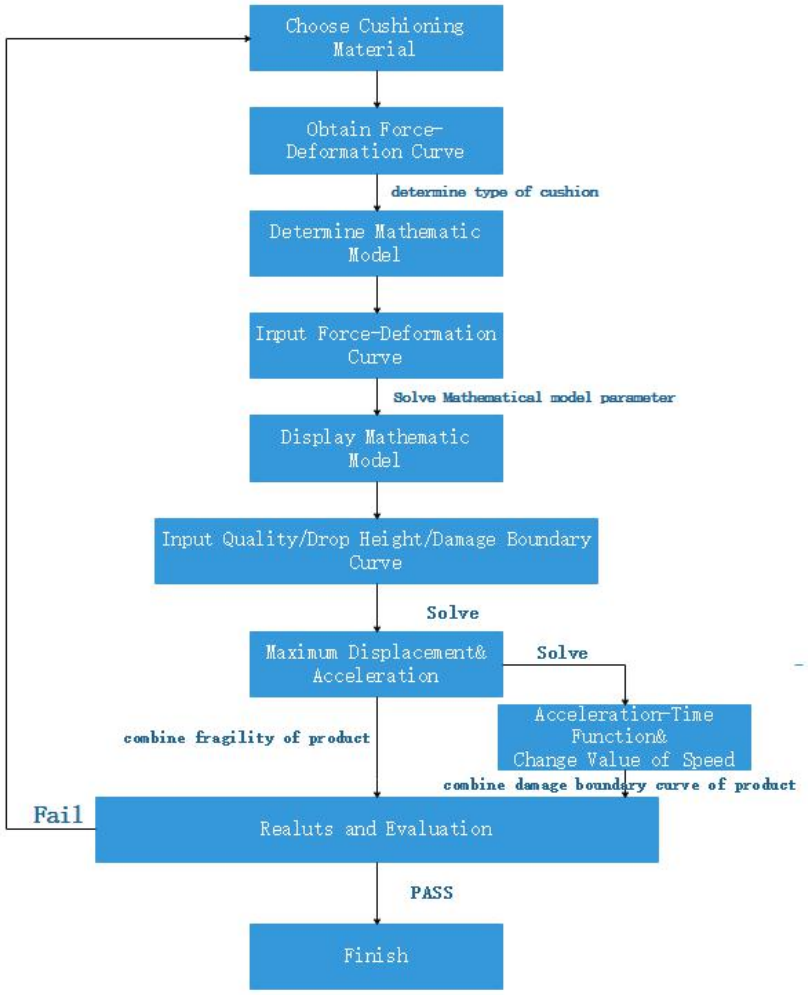

Figure 79. Flow Cart of Nonlinear Packaging Analysis

6.3. Numerical simulation analysis of cushioning packaging

The traditional method of packaging design is through mechanical experiments to determine the damage of the packing in different transportation environment. But the physical experiment of cushioning package is often destructive to the product, and the cost of the experiment is expensive, which limits the application of the traditional cushioning packaging design method.

With the help of computer numerical simulation, it is no need for prototyping packaging to drop test, it can inspect the dynamic response of products when different materials are in the same structure. Comparative analysis of the buffer performance of different packaging materials, can also be dynamic research products using materials of different structure of the same response when, to find the buffer cushion packaging material with better performance, low cost and more suitable for the transportation conditions of cushion packaging structure. Once the packaging model is established, if we want to change the cushioning packaging material, and do not need to remodel, we need to change the material parameters to carry out the simulation analysis of the new cushioning package. Some of the experiments with internal hard fragile parts detection products, computer simulation can simulation analysis of structure of the vulnerable component environment and transport packaging system, offer the foundation for the design and optimization of personnel to improve packaging design, product packaging simulation and optimization process is shown in Figure 80.

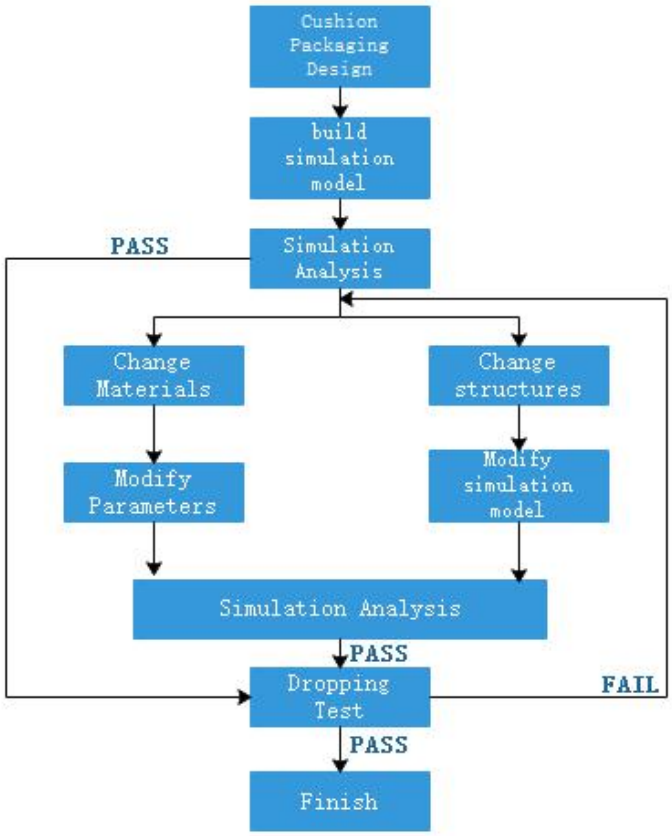

Figure 80. Flow Cart of the Packaging Drop Simulation

6.4. Cushion packaging design system

The traditional buffer packaging design method, nonlinear theory analysis method and numerical simulation analysis method have advantage and complement. This section talked about how to combine them to form a set of cushioning packaging design system, applied to the actual cushioning packaging design and made a preliminary exploration and discussion. Figure 81 shows the system block diagram of cushioning packaging design.

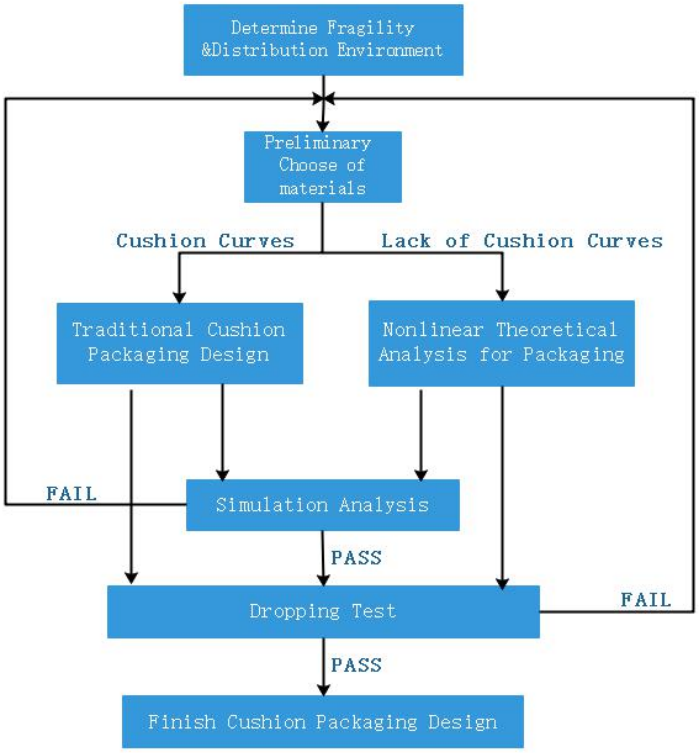

Figure 81. Cushion Design Principle of Packaging

As shown in Figure 81, the flow of cushioning packaging design, based on the design principles of specific circumstances, should reflect the following ideas:

First, according to the traditional cushioning packaging design principles, the main design parameters and the types of buffer materials are first determined:

1) Determine the crisp value of the product (or the broken boundary curve);
2) According to the distribution environment of the product, the drop height, temperature and humidity conditions of the product are determined;
3) Preliminary selection of suitable cushioning packaging materials.

Secondly, according to the requirement of the product, the appropriate design method of cushioning packaging is selected, and the preliminary cushion design is carried out.

Moreover, the simulation analysis is used to determine whether preliminary design of the cushion is suitable and the performance requirements can be met. Furthermore, the

prototype drop test of the cushioning package is carried out to determine whether the buffer design is qualified. Finally, improve the cushioning package design.

6.5. Conclusion

In this chapter, the application of nonlinear theoretical analysis and numerical simulation analysis of buffer packaging is discussed. The numerical simulation optimization process of product cushioning packaging is put forward. And the modern cushioning packaging design system is summarized, which provides the basis for the scientific and rational design of the cushioning package.

7. SUMMARY AND PROSPECT

7.1. Major Research Achievement

In this paper, the performance of cushioning packaging materials is studied by means of theoretical analysis and test. Based on in-depth study of the basic theory and design method of cushioning transport packaging, through theoretical analysis, simulation and experimental analysis, a comprehensive research on the cushioning packaging design methods was made. The design system and application method of buffering packaging are summarized. The following work is summarized as follows:

1) The mechanical properties and buffer efficiency of cushioning materials are mainly studied. The cushioning characteristic curves of these materials was drawn through the experiment, and the dynamic cushioning performance of the material was analyzed and compared. The scope of application and the selection principle of the material are given.

2) Based on theoretical deduction and experimental verification, a new method for determining the characteristic curve of packaging cushioning material is established. This method can effectively reduce the test times of material buffer characteristic curves, save much human and material resources, and set foundation for improving the performance curve library of cushioning packaging materials.

3) According to the stress-strain curve of the material, the effect of the plasticity and viscosity of the material on the material buffering performance is expounded. Based on establishing the mechanical model of cushioning pad and the integral equation of shock response for packages, a method for solving acceleration time function of products and vulnerable parts under nonlinear conditions is presented. Then, according to the theory of the impact brittleness value and the broken boundary curve of the product, the theoretical evaluation method of the rationality of the selection of the cushioning packaging material is explained.

4) Combined with the drop test of the package, a numerical simulation model for the drop impact of the cushioning package is set up. The method and steps of the finite element simulation analysis of the nonlinear buffer packaging system are given. The dynamic response process of the fall of the cushioning package is simulated, which provides a general simulation analysis method for the design of the cushioning transport package.

5) Combined with the specific product and its cushioning package, the experiment scheme for the drop test of the package is set up, and the concrete experimental steps are given. Finally, the drop impact test data are compared to simulation results, and reliability and practicability of the finite element analysis are verified.

7.2. Prospect and Development

The research work in this paper is still lacking in the following aspects and needs further development and deepening.

1) In this paper, the integral method is applied to nonlinear packaging materials, without the damping of the liner. But in the process of drop impact, the damping property of cushioning material is more obvious. It is necessary to consider the effect of material damping on material cushioning performance. Therefore, the drop impact response of the damping nonlinear packaging needs further study.

2) A new method for determining the material cushion curves are presented in this paper, only tested for polyethylene foam and foamed polystyrene foam cushioning material two. The method for other packaging materials commonly used are applicable, need to be further studied.

3) The computer simulation analysis model of nonlinear packaging is further perfected to make the model parameters closer to the real package.

4) Cushioning packaging design science must start from the product fragility, finite element analysis method can be used to determine the important parameters of crisp value, such as natural frequency of cushioning packaging design, as a cushion

packaging and packaging box design based on product design, and through the analysis of numerical simulation packages, to optimize the analysis cushioning packaging, avoid excessive packaging, save packing cost, make the research of cushioning packaging is more scientific and more reliable.

LIST OF REFERENCE

Andrae, A. S., & Andersen, O. 2010. Life cycle assessments of consumer electronics—are they consistent? The International Journal of Life Cycle Assessment, 15(8), Pp. 827-836.

Azzi, A., Battini, D., Persona, A., & Sgarbossa, F. 2012. Packaging design: general framework and research agenda. Packaging Technology and Science, 25(8), Pp.435-456.

Branson, D. E. & Christiason, M. L. 1971. Time Dependent Concrete Properties Related to Design-Strength and Elastic Properties, Creep, and Shrinkage. Special Publication, 27, Pp. 257-278.

Burgess, G. J. 1988. Product fragility and damage boundary theory. Packaging Technology and Science, 1(1), Pp. 5-10.

Cai, H.P. 2008. Packaging Introduction. Beijing: China Light Industry Publishing House. Pp. 22-25.

Chapman, S., & Cowling, T. G. (1970). The mathematical theory of non-uniform gases: an account of the kinetic theory of viscosity, thermal conduction and diffusion in gases. Cambridge university press. Pp.125-128.

Dominic, C. 2005. Integrating Packaging Suppliers into the Supply/Demand Chain. Packaging technology and science, 18, Pp.151-160.

Eagleton, D. & Marcondes, K. 1994. Cushioning properties of moulded pulp. Packaging Technology and Science, 7:2, Pp.65-72.

Edwards, M. E., & Good, T. A. 2001. Use of a mathematical model to estimate stress and strain during elevated pressure induced lamina cribrosa deformation. Current eye research, 23(3), Pp.215-225.

FMI (Future Market Insight). 2015. Consumer Electronics Market: Global Industry Analysis and Opportunity Assessment 2015 - 2020, Pp. 3-4.

GAO, D. 2005. The Property and Prospect of the Corrugated Paper Board. Packaging Engineering, 45(8), p.68.

Geuzaine, C., & Remacle, J. F. 2009. Gmsh: A 3‐D finite element mesh generator with built‐in pre‐and post‐processing facilities. International journal for numerical methods in engineering, 79(11), Pp.1309-1331.

Goyal, S., & Buratynski, E. K. 2000. Methods for realistic drop-testing. International journal of microcircuits and electronic packaging, 23(1), Pp.45-52.

Guo, Y., Xu, W., Fu, Y., & Zhang, W. 2010. Comparison studies on dynamic packaging properties of corrugated paperboard pads. Engineering, 2(05), p.378.

Hill, R. 1998. The mathematical theory of plasticity (Vol. 11). Oxford university press.Pp.68-72.

Huang, J. and Chen, L. 2002. Packaging Art Design. Chongqing: Chongqing University Publishing House,. p.218.

Kirwan, M. (2005). Paper and paperboard packaging technology. Oxford, UK: Blackwell Pub. p.89.

Landrock, A. H. 1995. Handbook of plastic foams: types, properties, manufacture and applications. Elsevier, 59(6), Pp.215-216.

Liu, G., Song, H. Y., 2005. The study on performance of air cushion mats. Packaging and Food Machinery, 82(6). Pp.58-59.

Lu, F. D., Tao, W. M., & Gao, D. 2013. Virtual mass method for solution of dynamic response of composite cushion packaging system. Packaging Technology and Science, 26(S1), Pp.32-42.

Ma, C., Wang, Y., Zou, G. 2015. The Main Factors that Influence the Mechanical Properties of Honeycomb Board. AMR, 1119, Pp.812-815.

Miltz, J., & Gruenbaum, G. 1981. Evaluation of cushioning properties of plastic foams from compressive measurements. Polymer Engineering & Science, 21(15), Pp.1010-1014.

Moaveni, S. 2011. Finite element analysis theory and application with ANSYS, 3/e. Pearson Education India. Pp.224-228.

Muskhelishvili, N. I. 2013. Some basic problems of the mathematical theory of elasticity. Springer Science & Business Media. Pp.161-165.

Newton, R. E. 1968. Fragility assessment theory and test procedure. Pp.118-136.

Olsson, A. & Györei, M. 2002. Packaging throughout the value chain in the customer perspective marketing mix. Packaging Technology and Science, 15(5), Pp. 231-239.

Ok, Y., & Sasaki, H. 2000. Social and environmental impacts of packaging (LCA and Assessment of packaging functions). Packaging technology and science, 13, pp.45-53.

Pan, M. C., & Chen, P. C. 2007. Drop simulation/experimental verification and shock resistance improvement of TFT–LCD monitors. Microelectronics Reliability, 47(12), Pp. 2249-2259.

Pecht, M. 1991. Handbook of electronic package design. New York: Marcel Dekker. Pp. 128-132.

Peng, G., 2006. Transport Packaging Design. Beijing: Printing Industry Publishing House. Pp.137-145. & p.65.

Porras-Hurtado, L., Ruiz, Y., Santos, C., Phillips, C., Carracedo, Á., & Lareu, M. 2013. An overview of STRUCTURE: applications, parameter settings, and supporting software. Frontiers in genetics, 4, p.98.

Rouillard, 2004. The dynamic behavior of stacked shipping units during transport. Part 1: model validation. Packaging Technology and Science, 17(5), Pp.237-247.

Rust, W., & Schweizerhof, K. 2003. Finite element limit load analysis of thin-walled structures by ANSYS (implicit), LS-DYNA (explicit) and in combination. Thin-walled structures, 41(2-3), Pp.227-244.

Saeed M., 2008. Finite Element Analysis Theory and Application with ANSYS. Third Edition, Publishing House of Electronics Industry, Beijing. Pp.144-147.

Sahoo, P., & Ghosh, N. 2007. Finite element contact analysis of fractal surfaces. Journal of Physics D: Applied Physics, 40(14), p.4245.

Sek, M. A., Minett, M., Rouillard, V., & Bruscella, B. 2000. A new method for the determination of cushion curves. Packaging Technology and Science, 13(6), Pp.249-255.

Sims, G. L. A., & Bennett, J. A. 1998. Cushioning performance of flexible polyurethane foams. Polymer Engineering & Science, 38(1), Pp.134-142.

Smithers Pira, 2015. The Future of Global Packaging to 2020. p.148

Sodhi, M. S., & Lee, S. 2007. An analysis of sources of risk in the consumer electronics industry. Journal of the Operational Research Society, 58(11), Pp.1430-1439.

Svanes, E., Vold, M., Møller, H., Pettersen, M. K., Larsen, H., & Hanssen, O. J. 2010. Sustainable packaging design: a holistic methodology for packaging design. Packaging Technology and Science, 23(3), Pp.161-175.

Wang, D. 2008. Experimental investigation into the cushioning properties of honeycomb paperboard. Packaging Technology and Science, 21(6), Pp.309-316.

Wang, Y. Y., & Lu, C., 2005. Simulation of drop/impact reliability for electronic devices. Finite elements in analysis and design, 41(6), Pp.667-680.

Wang, Z.W., Hu, C.Y., 1999, Shock spectra and damage boundary curves for nonlinear package cushioning system. Packaging Technology and Science, 12(5). Pp.37-42.

Wang, Z.W. 2001. Shock spectra and damage boundary curves for hyperbolic tangent cushioning system and their important features. Packaging Technology and Science, 14(4), Pp.149-157.

Wong, E. H., & Mai, Y. W. 2006. New insights into board level drop impact. Microelectronics reliability, 46(5-6), Pp.930-938.

YAN, L. R., & Xie, Y. 2010. Dynamic Cushioning Properties of Combination of Honeycomb Paperboard and EPE [J]. Packaging Engineering, 31(19), Pp.27-31.

Zeng, f. 2009. Development of electronic products transport packaging and existing problems. PACKAGING WORLD, 2009(01), Pp.43-49.